

**NASA CONTRACTOR  
REPORT**



N73-16605  
NASA CR-2192

NASA CR-2192

CASE FILE  
COPY

**AN INVESTIGATION OF  
THE SUTCLIFFE DEVELOPMENT THEORY**

*by Joseph Daniel Dushan*

*Prepared by*

**TEXAS A & M UNIVERSITY**

College Station, Texas

*for George C. Marshall Space Flight Center*

**NATIONAL AERONAUTICS AND SPACE ADMINISTRATION • WASHINGTON, D. C. • JANUARY 1973**

TECHNICAL REPORT STANDARD TITLE PAGE

1. REPORT NO. NASA CR-2192		2. GOVERNMENT ACCESSION NO.		3. RECIPIENT'S CATALOG NO.	
4. TITLE AND SUBTITLE AN INVESTIGATION OF THE SUTCLIFFE DEVELOPMENT THEORY				5. REPORT DATE January 1973	
				6. PERFORMING ORGANIZATION CODE	
7. AUTHOR(S) Joseph Daniel Dushan				8. PERFORMING ORGANIZATION REPORT # M107	
9. PERFORMING ORGANIZATION NAME AND ADDRESS Texas A & M University Department of Meteorology College Station, Texas				10. WORK UNIT NO.	
				11. CONTRACT OR GRANT NO. NAS 8-26751	
12. SPONSORING AGENCY NAME AND ADDRESS National Aeronautics and Space Administration Washington, D. C. 20546				13. TYPE OF REPORT & PERIOD COVERED  Contractor	
				14. SPONSORING AGENCY CODE	
15. SUPPLEMENTARY NOTES Submitted to the Graduate College of Texas A&M University in partial fulfillment of the requirements for the degree of Doctor of Philosophy.					
16. ABSTRACT Two case studies were used to test the Sutcliffe-Petterssen development theory for both cyclonic and anticyclonic development over the eastern United States. Each term was examined to determine when and where it made a significant contribution to the development process.  Results indicate the advection of vorticity at the level of non-divergence exerts the dominant influence for initial cyclone development, and that the thermal terms (advection of thickness, stability, and diabatic influence) become important after development has begun. Anticyclonic development, however, depends primarily on the stability term throughout the life cycle of the anticyclone.  Simple procedures for forecasting the development and movement of cyclones and anticyclones are listed. These rules indicate that routine National Meteorological Center analyses may be used to locate areas where the positive advection of 500-mb vorticity, indicative of cyclonic development, coincides with regions of severe weather activity. The development of anticyclones also is predicted easily. Regions of increasing stability, indicating anticyclonic development, may be located by use of National Meteorological Center radar summaries and analyses for 1000-500-mb thickness. A test of these techniques found them to be satisfactory for the case examined.					
17. KEY WORDS			18. DISTRIBUTION STATEMENT		
19. SECURITY CLASSIF. (of this report)  Unclassified		20. SECURITY CLASSIF. (of this page)  Unclassified		21. NO. OF PAGES  75	22. PRICE  \$5.00

## FOREWORD

This report is one of several to be published from research conducted under, or supported in part by, NASA Contract No. NAS8-26751, entitled "An Investigation of the Sutcliffe Development Theory." A number of approaches have been and continue to be followed in the conduct of the research. The results presented in this report are those from one approach, and represent only a portion of the total research effort. Other reports will be published as the research progresses.

## ACKNOWLEDGMENTS

The writer's graduate program was sponsored by the United States Air Force.

I wish to thank Dr. J. R. Scoggins for his guidance and continued encouragement during the study and preparation of this thesis, and Drs. R. A. Clark, V. E. Moyer, and W. S. McCulley for their comments and editorial assistance. Special appreciation goes to Major Philip W. West for aid with the computer programs.

The author gratefully acknowledges computer support provided by NASA under Contract No. NAS8-26751. This contract is under the auspices of the Aerospace Environment Division, Aero-Astrodynamic Laboratory, Marshall Space Flight Center, Huntsville, Alabama.

## TABLE OF CONTENTS

	Page
FOREWORD . . . . .	iii
ACKNOWLEDGMENTS. . . . .	iv
LIST OF FIGURES. . . . .	vii
LIST OF SYMBOLS. . . . .	x
1. INTRODUCTION . . . . .	1
2. BACKGROUND AND STATEMENT OF PROBLEM. . . . .	2
a. Theoretical Development. . . . .	2
b. Previous Studies . . . . .	5
c. Statement of the Problem . . . . .	7
d. Objectives of this Research. . . . .	8
3. ANALYTICAL APPROACH. . . . .	9
a. Grid System. . . . .	9
b. Evaluation of Terms in the Development Equation . . . . .	10
4. DESCRIPTION OF CASES AND RESULTS OF ANALYSIS . . . . .	16
a. Description of Case I, 5-8 December 1969 . . . . .	16
b. Results of Analysis for Case I . . . . .	19
c. Description of Case II, 1-4 November 1966 . . . . .	32
d. Results of Analysis for Case II. . . . .	35

TABLE OF CONTENTS (CONTINUED)

	Page
5. PRACTICAL UTILIZATION OF RESULTS . . . . .	46
a. Utilization of Facsimile Products . . . . .	46
b. Forecast Procedures . . . . .	47
c. Test of the Procedures . . . . .	49
6. SUMMARY AND CONCLUSIONS . . . . .	57
7. RECOMMENDATIONS FOR FURTHER RESEARCH . . . . .	59
LIST OF REFERENCES . . . . .	60

## LIST OF FIGURES

Figure		Page
1	Grid System used in computations . . . . .	10
2	Finite-difference grid used to evaluate the Laplacian . . . . .	12
3	Synoptic charts for 1000- and 500-mb levels for 0000 GMT, 5 December (top) and 1200 GMT, 6 December 1969 (bottom) . . . . .	17
4	Synoptic charts for 1000- and 500-mb levels for 0000 GMT, 7 December (top) and 0000 GMT, 8 December 1969 (bottom) . . . . .	18
5	Charts of 500-mb vorticity advection for 1200 GMT, 5-8 December 1969. . . . .	20
6	Charts of thickness advection term, and surface fronts for 1200 GMT, 5-8 December 1969. . . . .	22
7	Charts of 1000-500-mb thickness advection ( $10^{-3}$ m/sec) and surface fronts, for 1200 GMT, 5-8 December 1969 . . . . .	24
8	Charts of the stability term and areas of greatest diabatic influence for 1200 GMT, 5-8 December 1969. . . . .	26
9	Comparison of stability and severe weather activity for 1200 GMT, 5-8 December 1969. . . . .	28
10	Comparison of the computed vorticity tendency and the observed vorticity tendency for 1200 GMT, 5-8 December 1969 . . . . .	29

LIST OF FIGURES (CONTINUED)

Figure		Page
11	Time profiles of the 500-mb vorticity advection and the stability term over the cyclone center, 6-8 December 1969. . . . .	31
12	Synoptic charts for 1000- and 500-mb levels for 1200 GMT, 1 November (top) and 2 November 1966 (bottom). . . . .	33
13	Synoptic charts for 1000- and 500-mb levels for 1200 GMT, 3 November (top) and 4 November 1966 (bottom). . . . .	34
14	Charts of 500-mb vorticity advection for 0000 GMT, 1-4 November 1966. . . . .	36
15	Charts of 1000-500-mb thickness advection and surface fronts for 0000 GMT, 1-4 November 1966. . . . .	38
16	Comparison of analyses of stability and severe weather activity for 0000 GMT, 1-4 November 1966. . . . .	40
17	Comparison of the computed vorticity tendency and observed tendency for 0000 GMT, 1-4 November 1966. . . . .	42
18	Time profiles of the 500-mb vorticity advection and the stability term over the developing system, for (a) cyclonic development, 1-3 November 1966, and (b) anticyclonic development, 3-4 November 1966. . . . .	43

LIST OF FIGURES (CONTINUED)

Figure		Page
19	Copies of the NMC facsimile charts for 1200 GMT, 21 February 1971. . . . .	50
20	Copies of the NMC facsimile charts for 0000 GMT, 22 February 1971. . . . .	51
21	Copies of the NMC facsimile charts for 1200 GMT, 22 February 1971. . . . .	53
22	Copies of the NMC facsimile charts for 0000 GMT, 23 February 1971. . . . .	54
23	Time profile of 500-mb vorticity over the cyclone center for 21-23 February 1971. . . . .	55

## LIST OF SYMBOLS

$A_T$	advection of thickness
$A_Q$	advection of vorticity
$c_p$	specific heat at constant pressure
$D$	divergence
$f$	Coriolis parameter
$g$	acceleration of gravity
$H$	diabatic influence
$L$	latent heat
$P$	pressure
$P_0$	pressure at 1000 mb
$q$	relative vorticity
$q_T$	vorticity of the thermal wind
$Q$	absolute vorticity
$Q_0$	absolute vorticity at 1000 mb
$R$	gas constant of dry air
$S$	stability term
$S'$	any scalar quantity
$T$	temperature
$u, v$	components of wind velocity
$u_g, v_g$	components of geostrophic wind
$v$	wind speed
$v_0$	wind speed at 1000 mb
$v_T$	thermal wind speed

LIST OF SYMBOLS (CONTINUED)

$w_s$	saturation mixing ratio
$W$	heat
$Z$	height above sea level of an isobaric surface
$Z_0$	height above sea level of the 1000 mb surface
$\epsilon$	ratio of molecular weight of water to that of dry air
$\gamma_a, \gamma$	adiabatic and actual lapse rates in terms of height
$\Gamma_a, \Gamma$	adiabatic and actual lapse rates in terms of pressure
$\Gamma_s$	saturated adiabatic lapse rate
$\rho$	density
$\omega$	vertical velocity with pressure as vertical coordinate
$\vec{\nabla}$	del operator
$\nabla^2$	Laplacian operator

## 1. INTRODUCTION

One of the most important problems faced by synoptic meteorologists engaged in both short- and long-range forecasting is that of predicting accurately the development of cyclones and anti-cyclones at sea level. Techniques that would give the forecaster the ability to predict the location and general timing of such development would increase greatly the value of his product.

In the last 30 years, a considerable amount of study has been devoted to the theoretical aspects of cyclone development. In a series of papers, Sutcliffe (1939, 1947, 1950) formulated the problem of forecasting development in terms of vorticity changes and divergence, by use of Dines' compensation principle (Petterssen, 1956) which states that areas of divergence in the upper troposphere are balanced by similar areas of convergence in lower layers, and vice versa. Sutcliffe demonstrated that the magnitude of these compensating divergences, in both upper and lower levels, could be related to the geometry of the thermal pattern, thus indicating the vertical variation of vorticity transport.

---

The citations on the following pages follow the style of the Journal of Applied Meteorology.

## 2. BACKGROUND AND STATEMENT OF PROBLEM

Petterssen (1955, 1956) modified and extended Sutcliffe's theory with particular reference to the development of cyclones at sea level. He showed that cyclogenesis results from an imbalance between the advection of vorticity at the level of non-divergence (LND) and the Laplacian of certain thermal quantities below the LND.

### a. Theoretical Development

The vorticity equation with tilting neglected can be written in  $x, y, p, t$  coordinates (Petterssen, 1955), as

$$\frac{\partial Q}{\partial t} + u \frac{\partial Q}{\partial x} + v \frac{\partial Q}{\partial y} + \omega \frac{\partial Q}{\partial p} = -DQ, \quad (1)$$

where  $Q$  denotes the absolute vorticity and  $D$  denotes divergence.\*

The parameter  $\omega (= \frac{\Delta p}{\Delta t})$  is proportional to vertical motion, but opposite in sign; hereafter it will be referred to as vertical velocity. If the vertical advection of vorticity is assumed to be small; and is neglected, Eq. (1) becomes

$$\frac{\partial Q}{\partial t} = -\vec{v} \cdot \vec{\nabla} Q + \frac{\partial \omega}{\partial p} Q, \quad (2)$$

where

$$D = - \frac{\partial \omega}{\partial p}.$$

When Eq. (2) is applied at the LND,  $D = - \frac{\partial \omega}{\partial p} = 0$ , and

$$\frac{\partial Q}{\partial t} = -\vec{v} \cdot \vec{\nabla} Q.$$

\*See Appendix A

If  $\vec{V}_0$  is the wind at 1000 mb and  $\vec{V}_T$  the thermal wind from 1000 mb to the LND, then the wind at the LND is given by

$$\vec{V} = \vec{V}_0 + \vec{V}_T .$$

Similarly, we may write

$$Q = Q_0 + \delta\tau \quad \text{and} \quad \frac{\partial Q}{\partial p} = \frac{\partial \delta\tau}{\partial p} ,$$

where  $q_T$  is the vorticity of the thermal wind for the layer 1000 mb to the LND. By use of the above identities, the tendency of vorticity at 1000 mb may be written

$$\frac{\partial Q_0}{\partial t} = -\vec{V} \cdot \nabla Q - \frac{\partial \delta\tau}{\partial p} , \quad (3)$$

where the first term on the right-hand side (R.H.S.) refers to the LND.

Following Sutcliffe (1947), the first law of thermodynamics is used to find a convenient form for the term  $\frac{\partial \delta\tau}{\partial p}$ . Since pressure is the vertical coordinate, adiabatic (saturated or dry) and actual lapse rates in terms of pressure are expressed, respectively, as

$$\Gamma_a = \frac{1}{\rho g} \gamma_a \quad \text{and} \quad \Gamma = \frac{1}{\rho g} \gamma ,$$

where  $\rho$  denotes the density, and  $\gamma$  and  $\gamma_a$  denote lapse rates in terms of height. The first law of thermodynamics then may be written in the form

$$\frac{\partial T}{\partial t} = -\vec{v} \cdot \vec{\nabla} T + \omega(\overline{T_a} - \overline{T}) + \frac{1}{c_p} \frac{dW}{dt}, \quad (4)$$

where the three terms on the R.H.S. refer, respectively, to the horizontal advection of temperature, stability, and the heat (other than latent) supplied to or removed from the system.

The integration of Eq. (4) with respect to  $\log P$  from 1000 mb to the LND, after use of the hydrostatic relationship, yields

$$\frac{g}{R} \frac{\partial}{\partial t} (Z - Z_0) = \frac{g}{R} (\vec{v} \cdot \vec{\nabla} T) + \log\left(\frac{P_0}{P}\right) \left[ \overline{\omega(T_a - T)} + \frac{1}{c_p} \frac{dW}{dt} \right], \quad (5)$$

where  $Z - Z_0$  denotes the thickness of the layer,  $R$  is the gas constant for dry air, and  $c_p$  denotes the specific heat at constant pressure.

When the Laplacian of both sides is taken and terms are rearranged, Eq. (5) becomes

$$\frac{\partial g_T}{\partial t} = \frac{R}{f} \nabla^2 \left\{ \frac{g}{R} A_T + \log\left(\frac{P_0}{P}\right) \left[ \overline{\omega(T_a - T)} + \frac{1}{c_p} \frac{dW}{dt} \right] \right\}. \quad (6)$$

In this equation,  $f$  is the Coriolis parameter,  $g$  denotes the acceleration due to gravity, and  $A_T$  denotes the advection of thickness for the layer 1000 mb to the LND.

When the tendency of vorticity of the thermal wind, Eq. (6), is combined with Eq. (3), the tendency of vorticity at Earth's surface (or 1000 mb) may be written as

$$\frac{\partial Q_0}{\partial t} = \underset{\text{I}}{A_Q} - \underset{\text{II}}{\frac{R}{f}} \nabla^2 \left[ \underset{\text{III}}{\frac{g}{R}} A_T + \underset{\text{IV}}{S} + \underset{\text{V}}{H} \right], \quad (7)$$

where  $A_Q$  is the advection of vorticity at the LND,  $S = \left[ \log\left(\frac{p}{p_0}\right) \right] \left[ \overline{\omega(\bar{T}_a - \bar{T})} \right]$  is the stability, and  $H = \left[ \log\left(\frac{p_0}{p}\right) \right] \left[ \frac{1}{c_p} \frac{dW}{dt} \right]$  represents the contribution due to diabatic heating or cooling.

In the derivation of Eq. (7), motion was assumed to be adiabatic and frictionless. Geostrophic winds were used rather than actual winds and the level of non-divergence was assumed to be isobaric. The advection of vorticity at 1000 mb was found by Petterssen (1955, 1956) to make only a small contribution and, therefore, also was neglected. Thus, from Eq. (7), the tendency of vorticity at 1000 mb depends upon the horizontal advection of vorticity at the LND, and the Laplacian of the advection of thickness, stability, and thickness changes due to diabatic influences below the LND.

#### b. Previous Studies

With Petterssen's modified Sutcliffe theory as a basis, many experiments were conducted as regards forecasts of the development and intensification of extra-tropical cyclones. Because of the difficulty encountered in determining the adiabatic and diabatic changes of the temperature field by customary synoptic analysis, many investigators used a simplified approach wherein only the advection of vorticity at upper levels and thickness advection were considered as a measure of development.

Petterssen et al. (1955) tested the hypothesis that cyclogenesis occurs as a result of the superposition of an area of positive advection of vorticity at the LND on a surface frontal zone. Results indicated that the hypothesis was a useful forecast tool, but the advection of vorticity alone was not sufficient. To account for development at low altitudes, Petterssen and Bradbury (1954) used the advection of vorticity at 300 mb and the thermal advection below 300 mb. They found broad agreement with observed values, but numerical results were exaggerated by a factor of two to four.

Means (1955) conducted a similar study and, while his computed patterns agreed with those observed, the magnitudes were considerably overestimated. He concluded that, as a first approximation, the thermal advection in the layer between 1000 and 700 mb could be used in conjunction with the advection of vorticity at 300 mb as an indication of development.

Breistein (1954) determined that the advection of vorticity at 500 mb made the major contribution during the initial stages of development, and that the thermal effects became important after the occurrence of frontogenesis.

In an investigation of frictional effects during lee cyclogenesis, Newton (1955) found that the advection of vorticity alone was only a crude approximation of the development process. Brodrick and McClain (1969) showed that while the advection of cyclonic vorticity at 500 mb initially was a prime indicator of cyclone

development, thermal effects became increasingly important during later stages of cyclogenesis. Estoque (1956, 1957a, 1957b), Bradbury (1957), and others have used the Sutcliffe theory as modified by Petterssen to investigate wide-ranging topics such as vertical motion, stability, moisture, and cyclone models.

c. Statement of Problem

The many attempts at simplification of the Sutcliffe-Petterssen theory on development have suggested that to describe cyclogenesis and anticyclogenesis, consideration must be given to all of the terms, including the adiabatic and diabatic influences. These components, usually neglected by previous investigators, are interrelated with the advection of thickness and should not be considered as distinct physical processes.

Although the emphasis in all prior studies has been on cyclone development, the Sutcliffe-Petterssen theory applies to anticyclonic production as well. The application of the theory to the development of anticyclones also should be investigated.

In addition, it is of critical importance to present the results of any study of this nature in terms convenient for use by the practicing synoptic forecaster. Methods for predicting the development of cyclones and anticyclones, based on the Sutcliffe theory, should be devised. It is, after all, the ultimate goal of any meteorological research to improve the forecaster's product.

d. Objectives of this Research

The objectives of this research are to investigate examples of cyclogenesis and anticyclogenesis over the eastern United States, by use of the Sutcliffe development theory, as modified by Petterssen, and to determine when and where each term of the equation makes a significant contribution to cyclone development at sea level. In this study, all terms, including those assumed to be small and neglected by previous investigators, are examined. It is believed that this investigation presents a more extensive and detailed examination of the Sutcliffe theory than has been done previously. Finally, it is the aim of this research to present objective techniques to aid the weather forecaster in applying this theory in daily practice. These procedures take advantage of facsimile charts and analyses routinely available to the forecaster, and aid in the vital process of translating theoretical concepts into practical forecasting tools.

### 3. ANALYTICAL APPROACH

All data utilized in this research were 0000 and 1200 GMT rawinsonde (RAWIN) observations for stations east of the Rocky Mountains. The data were checked for hydrostatic consistency, and errors were resolved using checked radiosonde and rawinsonde data available on microfilm from the National Weather Records Center.

#### a. Grid System

To facilitate computation of parameters needed in the investigation, an 18 x 18 grid system was used (see Fig. 1). The grid points were 158.75 km apart, with the western edge of the grid placed along 105W longitude.

RAWIN data were interpolated to the grid points by use of a technique patterned after Barnes (1964). Basically, this is a method of successive corrections to a first-guess field initialized at zero. Observations were compared with the first-guess values at each grid point, and the differences were used to "correct" first-guess values. Four scans were made through the observations for each level and each parameter interpolated. The corrected grid then was smoothed to remove irregularities due to inherent "noise" in the data.

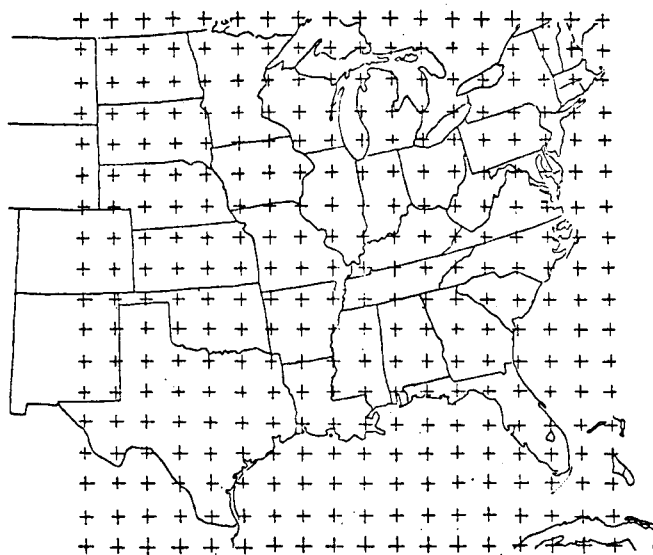


Fig. 1. Grid system used in computations.

b. Evaluation of Terms in the Development Equation

Computer programs were prepared for use on the IBM 360/65 computer to evaluate, by use of finite differences, each of the terms in Eq. (7). The LND was assumed to be constant and located at 500 mb. Observations indicate that, on the average, the LND is near 500 mb (Petterssen, 1955; Newton, 1956; Byers, 1959; Panofsky, 1964). In addition, vorticity analyses and forecasts of vorticity are available only at this level, and 1000-500 mb thickness patterns are routinely provided.

### 1) Advection of Vorticity at 500 mb

Relative and absolute vorticities were computed from the geostrophic wind components according to the following relationships

$$q = \frac{\partial v_g}{\partial x} - \frac{\partial u_g}{\partial y} \quad \text{and} \quad Q = q + f,$$

where

$$u_g = -\frac{g}{f} \frac{\partial Z}{\partial y} \quad \text{and} \quad v_g = \frac{g}{f} \frac{\partial Z}{\partial x}.$$

Here,  $\frac{\partial Z}{\partial y}$  and  $\frac{\partial Z}{\partial x}$  are the variations in height along the isobaric surface,  $q$  is the relative vorticity, and  $Q$  represents the absolute vorticity. The advection of vorticity at 500 mb, by components of the geostrophic wind at that level, was determined by

$$A_{500} = -u_g \frac{\partial Q}{\partial x} - v_g \frac{\partial Q}{\partial y},$$

where  $u_g$  and  $v_g$  are the components of the geostrophic wind, and

$\frac{\partial Q}{\partial x}$  and  $\frac{\partial Q}{\partial y}$  denote the variations in the 500-mb vorticity along the isobaric surface.

### 2) Laplacian of Thickness Advection

The thickness, or depth, of the 1000-500-mb layer is given by the difference in height above sea level of the two surfaces. The geostrophic wind at 700 mb was used to advect the computed values of thickness.

The Laplacian of the advection of thickness was evaluated using finite differences according to the relationship (Panofsky, 1964)

$$\nabla^2 S' = \frac{S'_1 + S'_2 + S'_3 + S'_4 - 4 S'_0}{H^2}$$

where S may be any scalar quantity (see Fig. 2). The thickness advection term then was determined by multiplying the factor  $-\frac{g}{f}$  by the value of the Laplacian of thickness advection at each grid point.

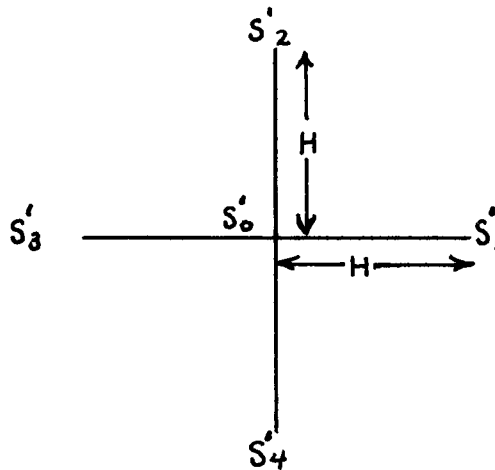


Fig. 2. Finite-difference grid used to evaluate the Laplacian. (H = 158.75 km.)

### 3) Stability Term

The stability term depends upon the mean value of the product of the stability factor,  $(\Gamma_a - \Gamma)$ , and the vertical motion,  $\omega$ , from 1000 to 500 mb.

To evaluate vertical motion, velocity divergence given by

$$D = - \frac{\partial \omega}{\partial p},$$

may be integrated between two levels to yield

$$\omega - \omega_0 = -\bar{D} (P - P_0),$$

or

$$\bar{\omega} = \bar{\omega}_0 - \bar{D}(P - P_0).$$

Vertical motion was computed at 850, 700, 500, and 400 mb, while at 1000 mb it was assumed to be zero. Divergence was computed from the actual wind according to the relationship

$$D = \frac{\partial u}{\partial x} + \frac{\partial v}{\partial y}.$$

The stability factor,  $(\Gamma_a - \Gamma)$ , was determined for the layers 1000-850 mb, 850-700 mb, and 700-500 mb.

Adiabatic lapse rates were assumed to be saturated if the temperature-dew-point depression was less than 3C, and upward vertical velocity ( $-\omega$ ) was greater than  $10^{-3}$  mb/sec through the layer. If these conditions were met, the saturated adiabatic lapse rate was computed by

$$\Gamma_s = \frac{g}{C_p} \left[ \frac{1 + \frac{L w_s}{R T}}{1 + \frac{\epsilon L^2 w_s}{C_p R T^2}} \right],$$

where  $L$  is the latent heat,  $w_s$  is the saturation mixing ratio,  $\epsilon$  is the ratio of the molecular weight of water to that of dry air,  $R_d$  is the gas constant for dry air, and  $T$  is the air temperature (Hess, 1959).

When conditions for saturation were not fulfilled, the adiabatic lapse rate was considered to be dry and  $\Gamma_a$  was assigned the standard value of 10C per km. The actual lapse rate of temperature,  $\Gamma$ , was computed by

$$\Gamma = - \frac{1}{\rho g} \left( \frac{T - T_0}{\Delta P} \right),$$

where  $T$  and  $T_0$  refer to the observed temperatures at the top and bottom of the layer, respectively, and  $\Delta P$  is the thickness of the layer. The two components,  $\omega$  and  $(\Gamma_a - \Gamma)$ , were used to determine the stability for the layer 1000-500 mb, and the stability term was calculated by multiplying the factor  $-\frac{R}{f}$  by the Laplacian of the stability. (See Eq. (6).)

#### 4) Diabatic Influence

The diabatic contribution was evaluated by computation of the difference between the actual 12-hour change in the 1000-mb vorticity, and terms II, III, and IV in Eq. (7). The difference was assumed to be due mainly to diabatic influences. It is understood,

however, that this is not entirely accurate. In addition to diabatic influences, the result contains contributions from previously neglected terms, such as friction, tilting (neglected in vorticity calculations), and assumptions used in the computation of vertical velocities and lapse rates of temperature for the stability term. This method does, however, indicate areas of relative diabatic influence.

#### 5) Vertical Transport of Vorticity Through the LND

This term, neglected in vorticity calculations by previous investigators, was determined by use of the relationship

$$\omega \frac{\partial Q}{\partial P} = \frac{-\omega_{500} (Q_{400} - Q_{600})}{\Delta P},$$

where  $\omega_{500}$  is the vertical velocity at the 500-mb level, and  $Q_{400}$  and  $Q_{600}$  refer to absolute vorticities at 400 mb and 600 mb, respectively.

#### 4. DESCRIPTION OF CASES AND RESULTS OF ANALYSIS

Two separate synoptic situations were chosen for investigation. The two series, each of 4 days duration, provided examples of cyclonic and anticyclonic development, maturation, and decay. The only conditions for selection were that, as far as possible, the complete life cycle of the system occur within the grid system. This restriction was set to insure that adequate data were available.

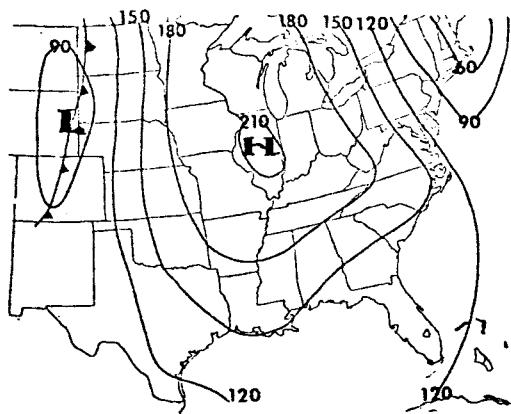
##### a. Description of Case I, 5-8 December 1969

On 5 December 1969 a shallow depression began to form at the surface on a weak cold front which moved into the Central Plains behind a high-pressure system centered over the upper Mississippi Valley. At upper levels, a trough at 500 mb pushed southeastward behind the surface cold front (Figs. 3a and 3b).

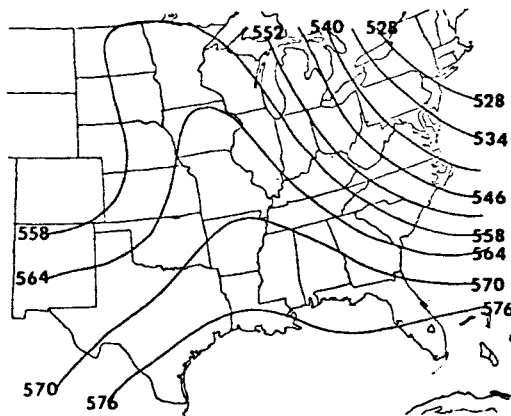
By 1200 GMT on 6 December (Figs. 3c and 3d), a closed system had formed in the western Gulf of Mexico as the axis of the deepening 500-mb trough moved over the cold front through southern Texas. During this time, the circulation around the low center increased as the low deepened 90 m at 1000 mb.

During the next 12 hours, as the upper trough continued to move eastward, the circulation increased and the surface cyclone underwent its most rapid development, and by 0000 GMT on 7 December, the mature system was centered over Louisiana (Figs. 4a and 4b).

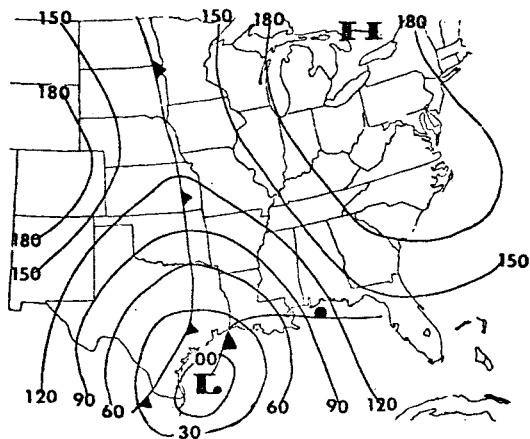
In the next 24 hours, the axis of the upper trough (500 mb) moved over the surface cyclone, as the system moved northward



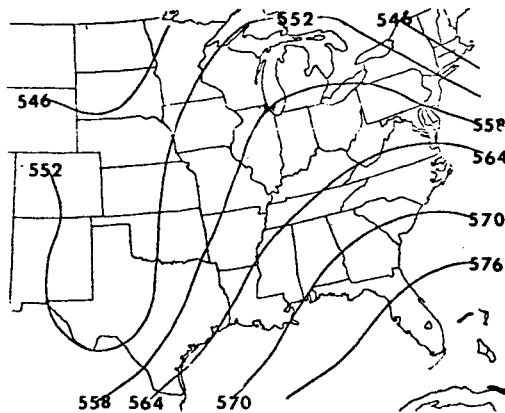
(a) 1000 mb



(b) 500 mb

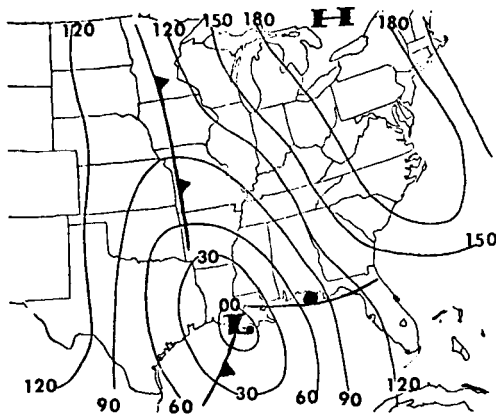


(c) 1000 mb

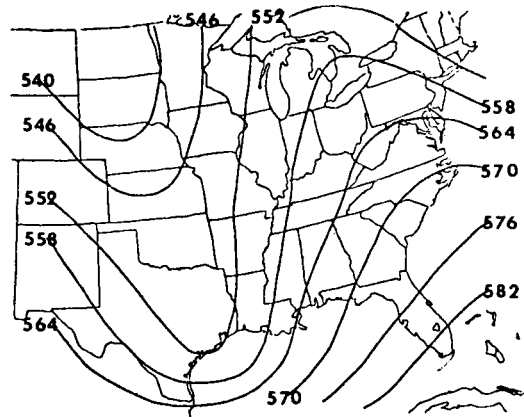


(d) 500 mb

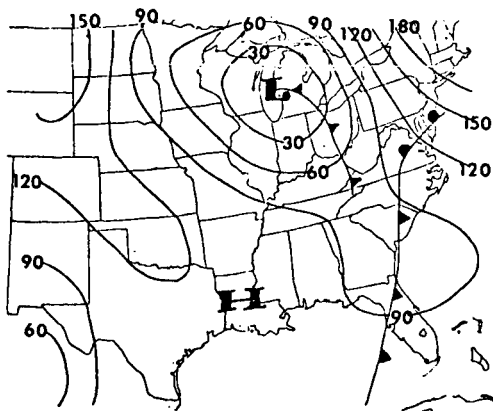
Fig. 3. Synoptic charts for 1000- and 500-mb levels for 0000 GMT, 5 December (top) and 1200 GMT, 6 December 1969 (bottom).



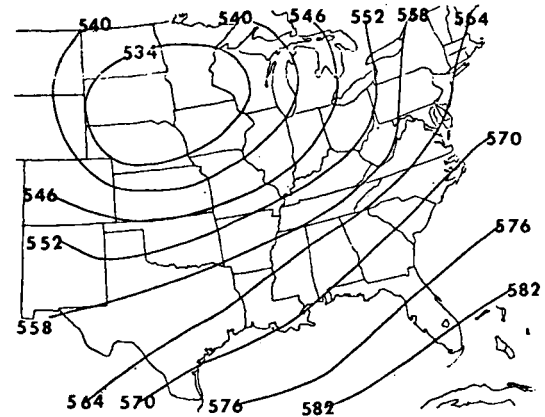
(a) 1000 mb



(b) 500 mb



(c) 1000 mb



(d) 500 mb

Fig. 4. Synoptic charts for 1000- and 500-mb levels for 0000 GMT, 7 December (top) and 0000 GMT, 8 December 1969 (bottom).

through the Mississippi Valley and circulation decreased around the filling low center. Meanwhile, high pressure was developing over the south central United States (Figs. 4c and 4d).

By 1200 GMT on 8 December, the low center was located over the western Great Lakes and high pressure continued to dominate the south central portion of the United States.

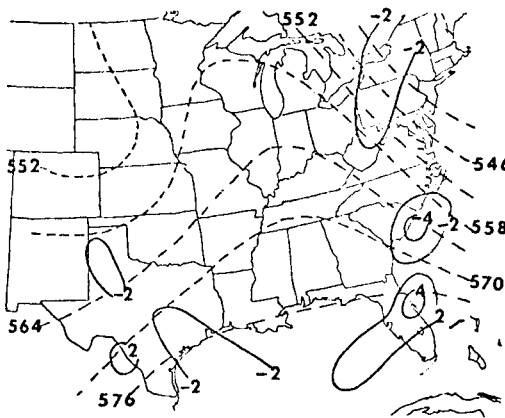
b. Results of Analysis for Case I

Scalar fields of the terms discussed in Section 3b were analyzed to determine the contribution to development made by each parameter.

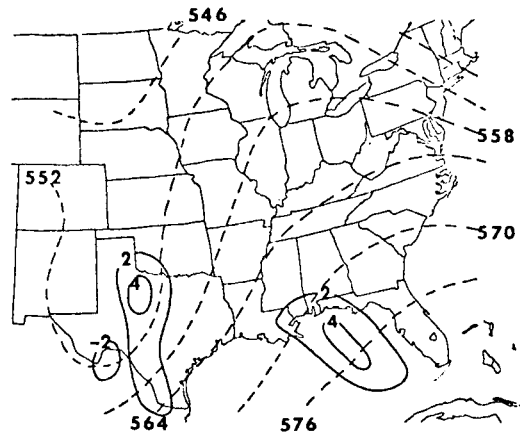
1) Advection of 500-mb Vorticity (Term I, Eq. (7))

The advection of 500-mb vorticity at 1200 GMT each day is shown in Fig. 5. Positive values indicate positive vorticity advection while negative values indicate negative vorticity advection. During the initial stages of cyclogenesis over Texas (Fig. 5a), the advection of 500-mb vorticity was anticyclonic, though magnitudes were quite small. As the low center intensified and moved from Texas to the western Gulf of Mexico, cyclonic vorticity advection increased over Texas, as the associated upper trough (500 mb) deepened and its axis then moved eastward behind the surface low-pressure system (Fig. 5b). Although the cyclonic vorticity advection increased, the maximum values remained behind the developing system.

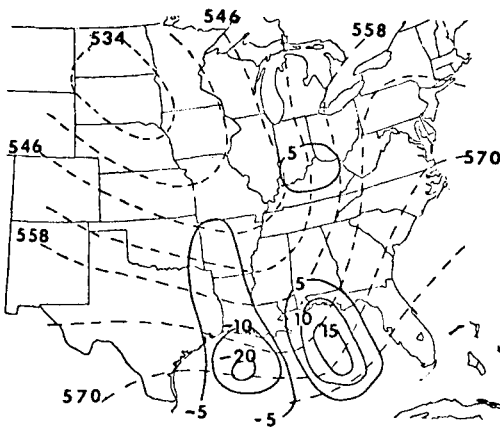
By 0000 GMT on 7 December, the magnitude of the maximum positive advection of vorticity increased from  $4 \times 10^{-9} \text{ sec}^{-2}$  to



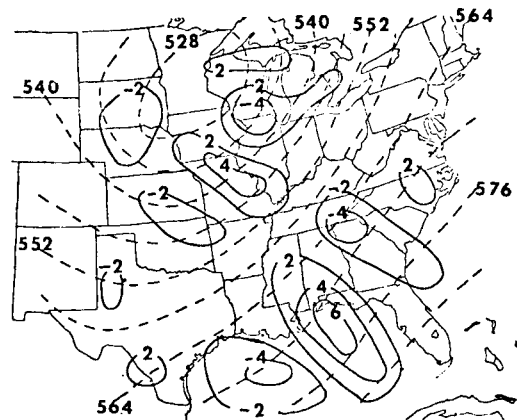
(a) 5 December 1969



(b) 6 December 1969



(c) 7 December 1969



(d) 8 December 1969

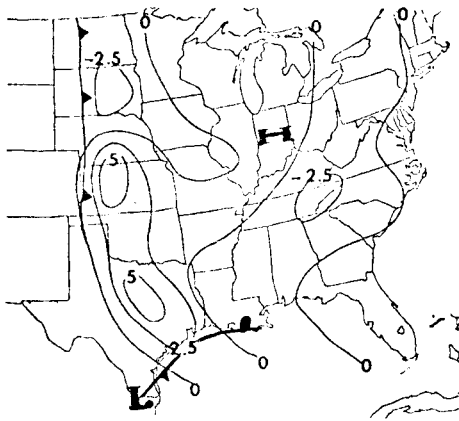
Fig. 5. Charts of 500-mb vorticity advection for 1200 GMT, 5-8 December 1969. Dashed lines indicate 500-mb height contours and solid lines represent 500-mb vorticity advection (units:  $10^{-9} \text{ sec}^{-2}$ ).

$20 \times 10^{-9} \text{ sec}^{-2}$  and was situated over the storm center. This corresponds to the time of greatest development. By 1200 GMT, the low center had moved from Louisiana to Illinois and the axis of the 500-mb trough was over the low center, with positive vorticity advection ahead of the storm. Over the cyclone, the advection was still positive, but had decreased to  $5 \times 10^{-9} \text{ sec}^{-2}$  (Fig. 5c). The maximum positive advection of vorticity at this time was east of the upper trough over the eastern Gulf of Mexico. Although the low center was well to the north, this area corresponded to an elongation of the surface trough through Alabama.

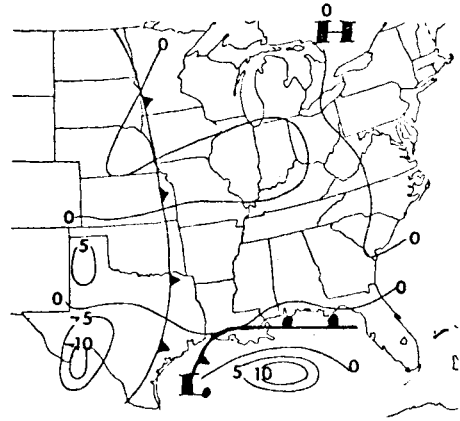
By 1200 GMT on 8 December, the low had moved to the western Great Lakes and had started to weaken. The positive advection of vorticity over the low decreased from  $5 \times 10^{-9} \text{ sec}^{-2}$  to  $2 \times 10^{-9} \text{ sec}^{-2}$  over the center (Fig. 5d). The greatest positive advection still was over the eastern Gulf of Mexico, though magnitudes decreased by over 50%, as the surface trough filled and moved eastward. The advection of 500-mb vorticity was near zero in association with the dissipating high-pressure system over the Great Lakes region (Figs. 5a and 5b), and also with the developing anticyclone over the south central United States (Figs. 5c and 5d).

## 2) Thickness Advection Term (Term III, Eq. (7))

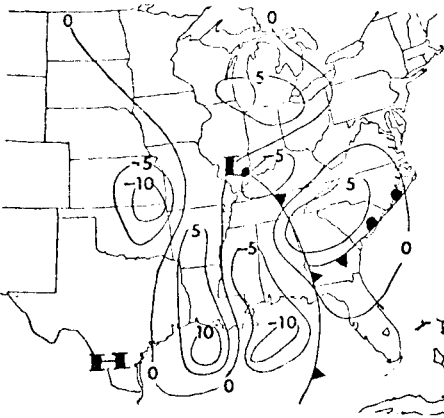
The contributions of the thickness advection term are shown in Fig. 6 for 1200 GMT each day. During all stages of cyclone development, the magnitudes of the term are near zero over the low-pressure center itself, with positive values to the rear.



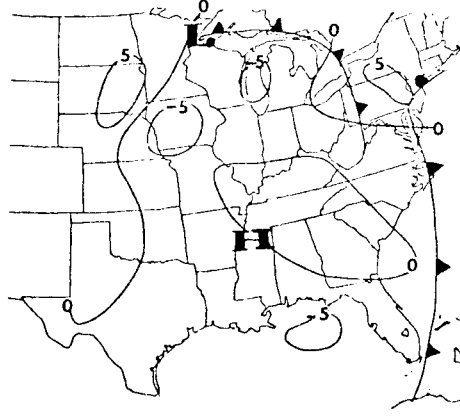
(a) 5 December 1969



(b) 6 December 1969



(c) 7 December 1969



(d) 8 December 1969

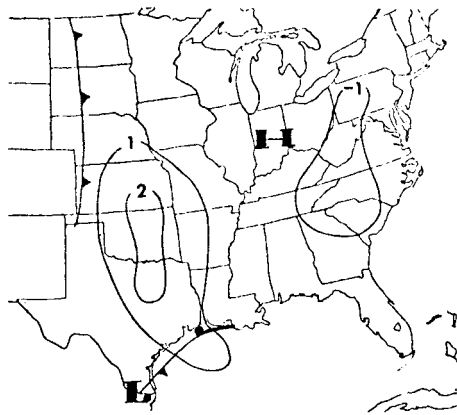
Fig. 6. Charts of thickness advection term, and surface fronts for 1200 GMT, 5-8 December 1969.

On 5 December, as the low began its initial development over Texas, a large area of positive thickness advection was observed from Kansas through Texas, ahead of the surface cold front (Fig. 6a). As the developing low center moved from Texas into the western Gulf of Mexico, positive and negative regions had developed ahead of and behind the storm, respectively (Fig. 6b).

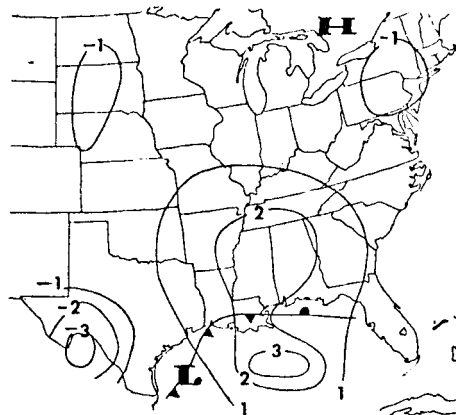
At 1200 GMT on 7 December, with the cyclone centered over Illinois, the magnitudes of the thickness advection term increased over the eastern United States (Fig. 6c), and remained large over the central Gulf of Mexico, in the southern portion of the surface trough. By 1200 GMT on 8 December, magnitudes of the term had decreased around the weakening cyclone center, then located over the western Great Lakes region (Fig. 6d).

The advection-of-thickness term for anticyclonic development is characterized by negative values in advance and positive values behind the system, with near-zero values over the center. As in the case of the contribution due to the advection of vorticity, the magnitudes of the thickness advection term for anticyclonic development and dissipation are quite small.

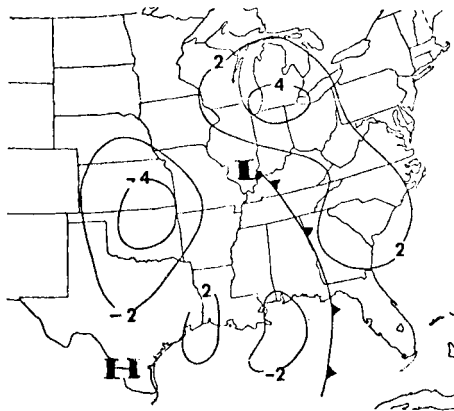
For comparison, Fig. 7 depicts the patterns of the advection of 1000-500-mb thickness before application of the Laplacian operator and constants. It can be seen that maximum and minimum values occur in the same geographical locations, but the magnitudes of the thickness advection term (Term III in Eq. (7)) are slightly larger.



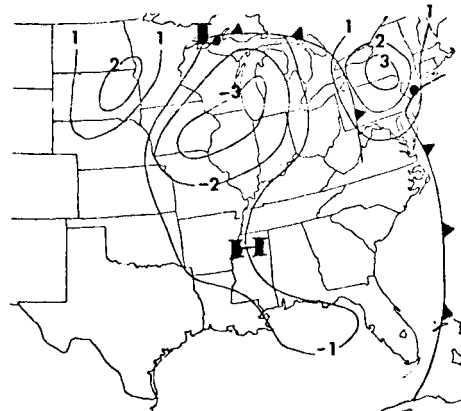
(a) 5 December 1969



(b) 6 December 1969



(c) 7 December 1969



(d) 8 December 1969

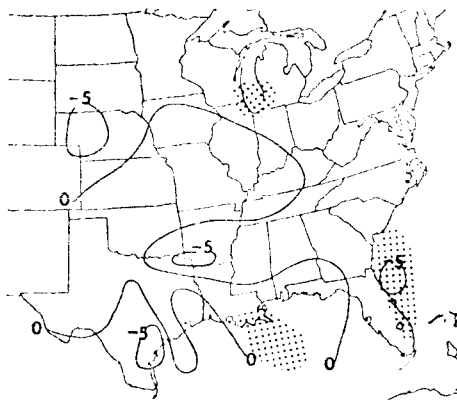
Fig. 7. Charts of 1000-500-mb thickness advection ( $10^{-3}$  m/sec) and surface fronts, for 1200 GMT, 5-8 December 1969.

### 3) Stability Term and Diabatic Influence

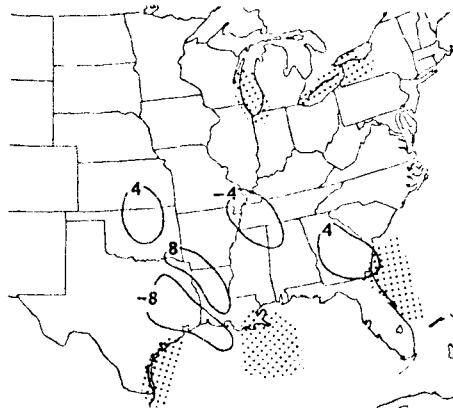
(Terms IV and V, Eq. (7))

The contributions due to stability and the diabatic influence are shown in Fig. 8 for 1200 GMT each day. Negative values of the stability term represent instability (cyclonic contribution), and vice versa, while stippled areas show regions of greatest diabatic influence. On 5 December, during the first stages of cyclone development, the low-pressure system over Texas was in a stable region (Fig. 8a). During the next 24 hours, the low center moved into the western Gulf of Mexico and stability decreased, enhancing further development. An additional factor for development was provided by the diabatic influence along the coastal areas of the Gulf of Mexico (Fig. 8b). By 1200 GMT on 7 December, the low center had moved into more stable air over Illinois and further intensification was retarded (Fig. 8c).

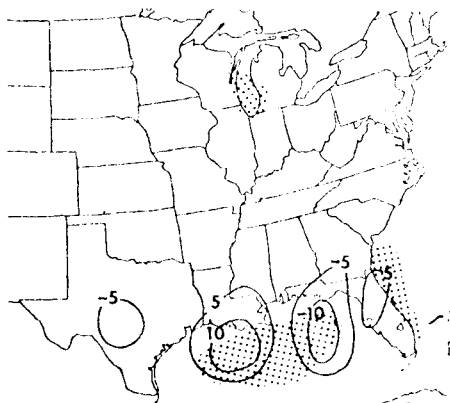
Continued development of the low was halted and the trough began to fill during the next 24 hours, as the low moved over the western Great Lakes. The diabatic contribution to development, present over Lake Michigan, was offset by increasing stability through the area (Fig. 8d). The stability term appears to be especially critical in the case of anticyclonic development. For example, decreasing values of the stability term over the central United States on 5 and 6 December correspond well with the north-eastward movement and dissipation of the ridge over the southern Great Lakes region as shown in (Figs. 3a and 3b, p. 17). Similarly,



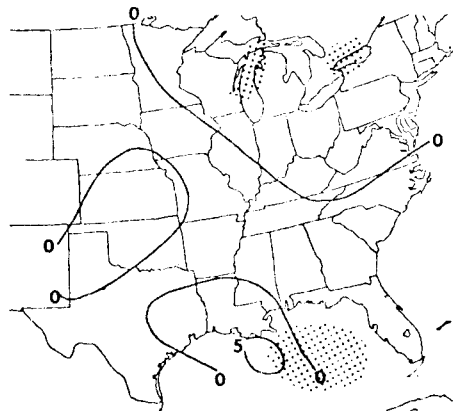
(a) 5 December 1969



(b) 6 December 1969



(c) 7 December 1969



(d) 8 December 1969

Fig. 8. Charts of the stability term and areas of greatest diabatic influence for 1200 GMT, 5-8 December 1969. (Solid lines represent contours of the stability term ( $10^{-9} \text{ sec}^{-2}$ ) and stippled areas show regions of greatest diabatic contributions. Negative values of the stability term indicate cyclonic contributions and positive values correspond to anticyclonic contributions.)

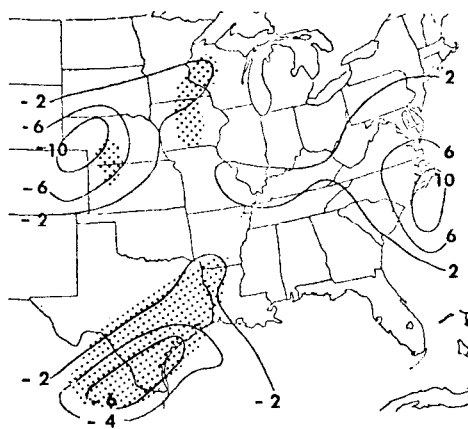
increasingly stable conditions through the southern portions of the country precede the developing anticyclone over the south central United States on 7 and 8 December (Figs. 3c and 3d, p. 17).

By comparison, Fig. 9 shows the patterns of stability before application of the Laplacian operator and constants. Stippled areas represent regions of severe weather activity depicted on National Meteorological Center (NMC) radar summaries, valid at the same times. It can be seen that areas of severe weather correspond well with areas of greatest instability, and that maximum and minimum values occur in the same geographical locations, before and after application of the Laplacian operator and constants.

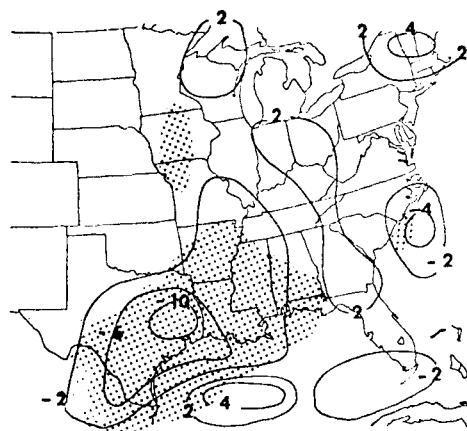
#### 4) Vorticity Tendency at 1000 mb (Term I, Eq. (7))

The tendency of vorticity at 1000 mb, computed by use of terms II, III, and IV in Eq. (7), with the diabatic influence neglected (term V), is shown in Fig. 10 for 1200 GMT each day. For comparison, the observed tendencies of 1000-mb vorticity, obtained by use of 12-hour changes in the actual 1000-mb vorticity, also are shown. Positive values of the tendency correspond to cyclonic development, while negative values indicate anticyclonic development.

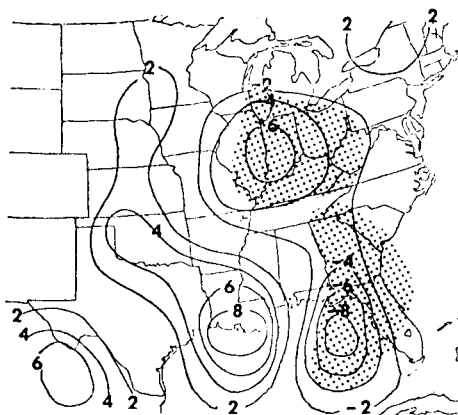
As may be seen, the patterns of the computed tendencies agree reasonably well with observed patterns, however the magnitudes of the computed values are, at times, one order of magnitude larger than those observed.



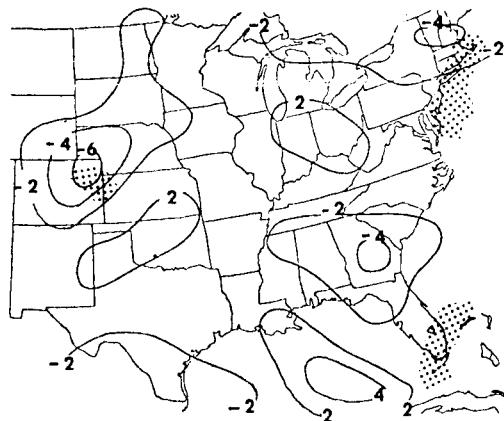
(a) 5 December 1969



(b) 6 December 1969

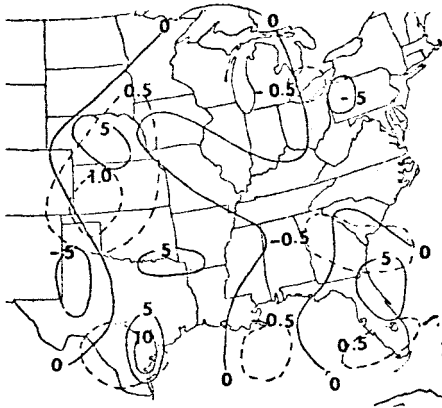


(c) 7 December 1969

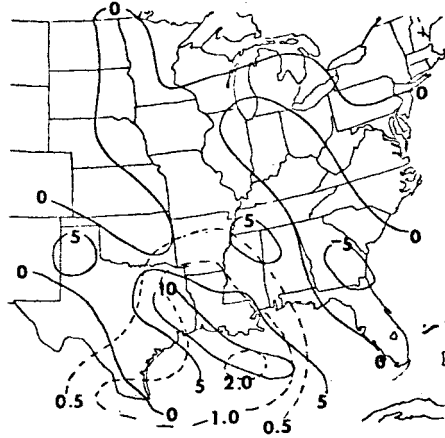


(c) 8 December 1969

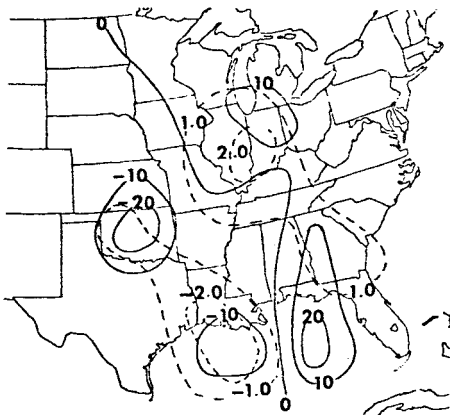
Fig. 9. Comparison of stability and severe weather activity for 1200 GMT, 5-8 December 1969. (Solid lines indicate stability contours and stippled areas correspond to severe weather echoes reported on NMC radar summaries.)



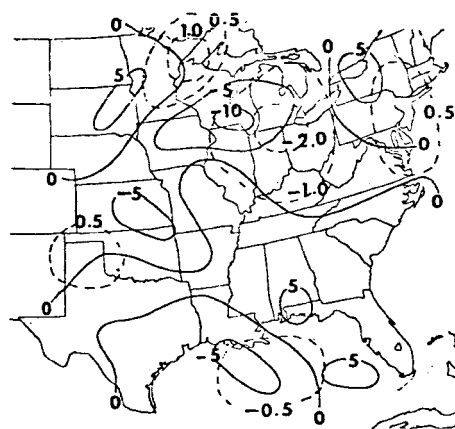
(a) 5 December 1969



(b) 6 December 1969



(c) 7 December 1969



(d) 8 December 1969

Fig. 10. Comparison of the computed vorticity tendency and the observed vorticity tendency for 1200 GMT, 5-8 December 1969. (Solid lines indicate contours of the computed tendency ( $10^{-9} \text{ sec}^{-2}$ ) and dashed lines show patterns of the observed tendency ( $10^{-9} \text{ sec}^{-2}$ ). Positive values correspond to cyclonic development and negative values indicate anticyclonic development.)

Contributions from the advection of vorticity at 1000 mb and the vertical transport of vorticity through the 500-mb level (LND), neglected by Petterssen and other investigators, are very small. Over the developing system, values for both terms are at least one order of magnitude less than terms II, III, and IV in Eq. (7), and may be neglected safely in this case.

The results for this synoptic case indicate that for cyclonic development, the advection of positive vorticity at 500 mb (LND) is the dominant factor during the early stages (Fig. 11). After the initial development of the cyclone has begun, cloud patterns form and the thermal influences, primarily stability, become more significant. The most intense development occurs when increasing contributions from positive vorticity advection and stability coincide over the surface center. The further intensification of the cyclone is retarded when these contributions decrease. Since the magnitude of the advection-of-thickness term is near zero over the storm, positive in advance and negative to the rear, this component appears to affect the movement of the developing system. The significant diabatic contributions, in this case, are restricted to coastal areas along the Gulf of Mexico and over the Great Lakes region, and over these locations cyclone development is enhanced.

The stability term appears to be the most important influence for both positive and negative anticyclonic development, in this case. Contributions from the advection of negative vorticity at

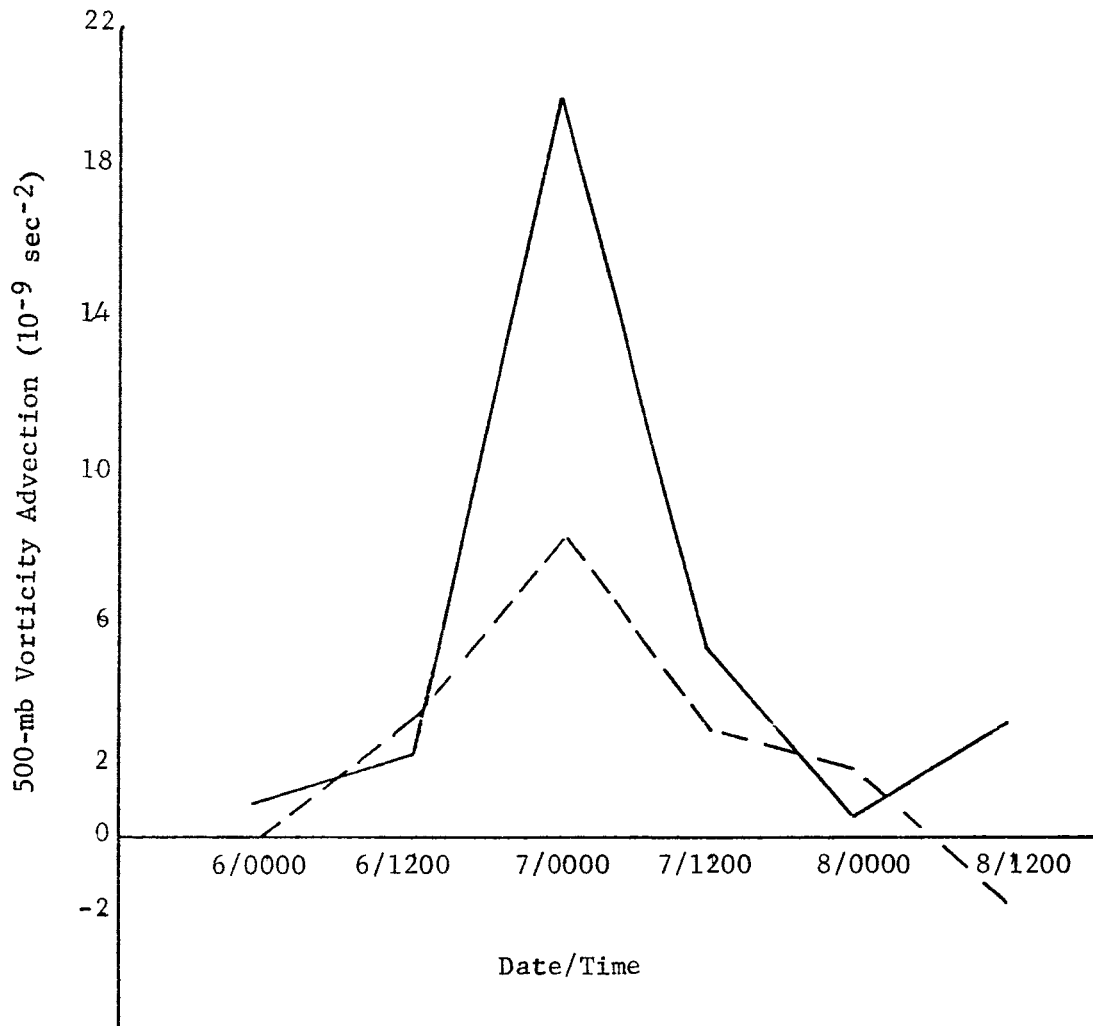


Fig. 11. Time profiles of the 500-mb vorticity advection and the stability term over the cyclone center, 6-8 December 1969. (The solid line shows vorticity advection and the dashed line indicates the stability term.)

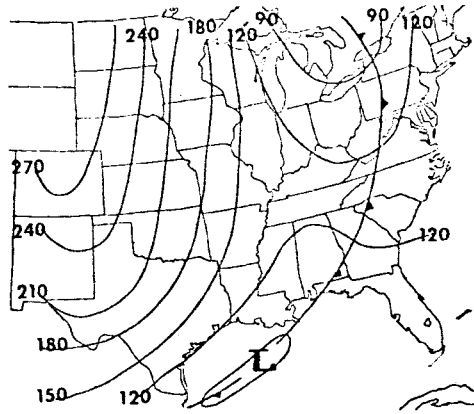
500 mb are very small. The advection-of-thickness term is near zero over the high-pressure center, with negative values in advance and positive values behind, but unlike the cyclone situation, patterns are relatively weak and magnitudes are small.

c. Description of Case II, 1-4 November 1966

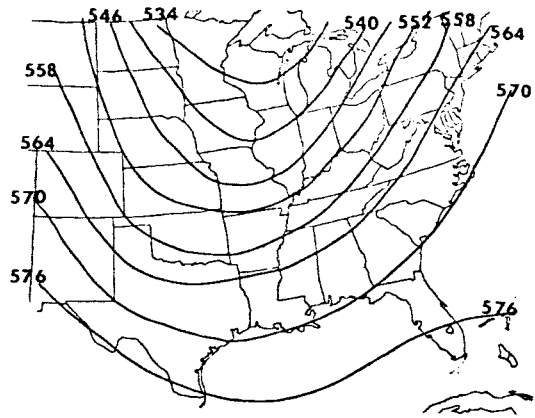
On 1 November 1966, a cyclone began to form in the upper troposphere, and by 1200 GMT a low center appeared at the surface in the central Gulf of Mexico associated with a cold front which stretched from the eastern Great Lakes to southern Texas. A trough at 500 mb moved slowly eastward behind the developing surface cyclone (Figs. 12a and 12b). Throughout the next day, the circulation around the system intensified and the low-pressure system deepened 60 m as it traveled through the eastern Gulf of Mexico to a position over the Carolinas (Figs. 12c and 12d). The 500-mb trough deepened rapidly and its axis moved eastward behind the surface disturbance.

Early on 3 November (Greenwich time), the pattern at 500-mb became closed and by 1200 GMT had moved over the surface cyclone, located over the Great Lakes, where development continued. The low deepened another 30 m at 1000 mb and strong circulation was observed.

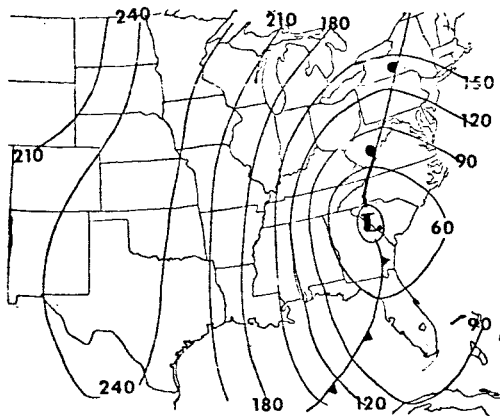
Meanwhile, high pressure was building over the western Gulf of Mexico and the south central United States (Figs. 13a and 13b). By 1200 GMT on 4 November, the low-pressure system had moved into eastern Canada, and developing high pressure, centered over



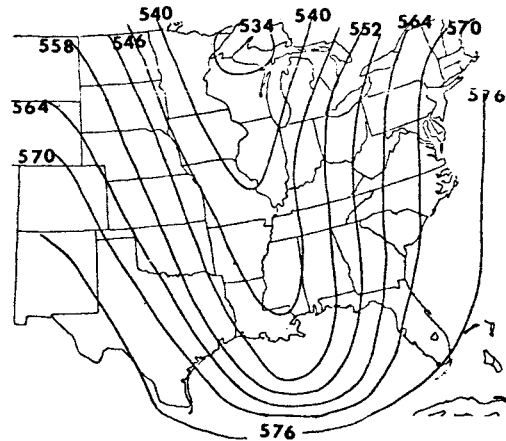
(a) 1000 mb



(b) 500 mb

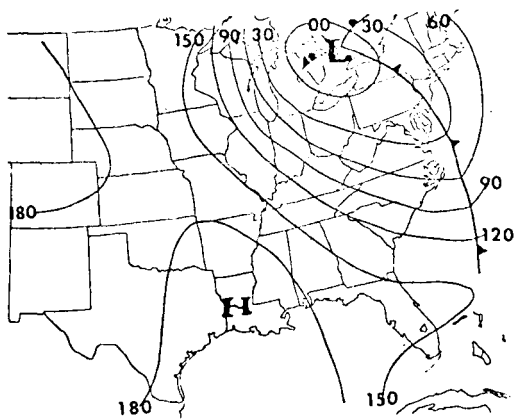


(c) 1000 mb

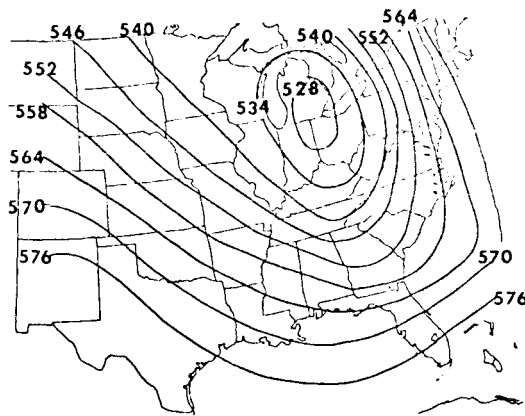


(d) 500 mb

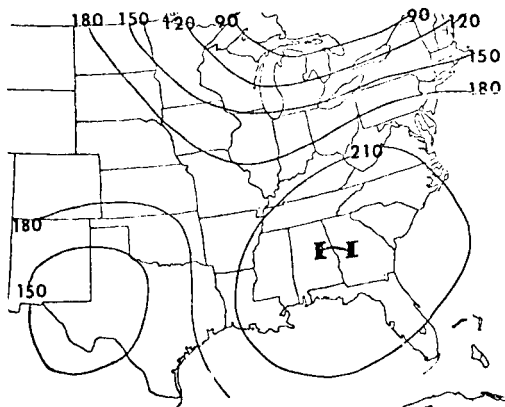
Fig. 12. Synoptic charts for 1000- and 500-mb levels for 1200 GMT, 1 November (top) and 2 November 1966 (bottom).



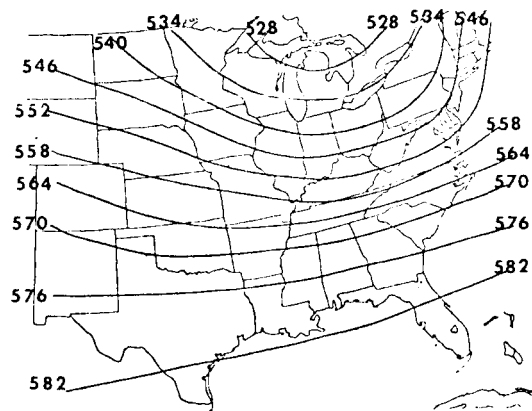
(a) 1000 mb



(b) 500 mb



(c) 1000 mb



(d) 500 mb

Fig. 13. Synoptic charts for 1000- and 500-mb levels for 1200 GMT, 3 November (top) and 4 November 1966 (bottom).

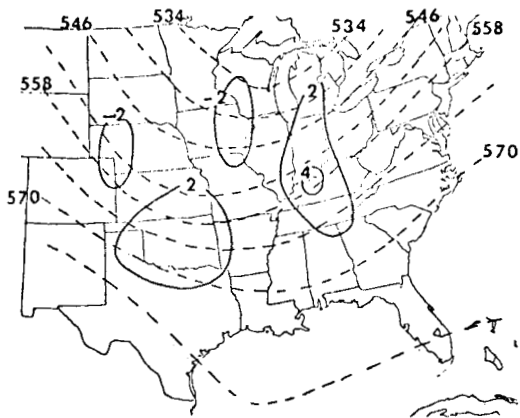
Georgia, dominated the southern portion of the country (Figs. 13c and 13d).

d. Results of Analysis for Case II

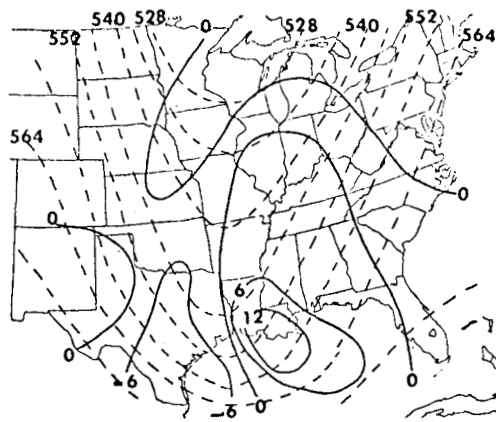
1) Advection of 500-mb Vorticity (Term II, Eq. (7))

Figure 14 shows the results of the analysis for the advection of vorticity at 500 mb at 0000 GMT, 1-4 November 1966. As the low-pressure center began to form and move across Texas to the central Gulf of Mexico, the positive advection of vorticity through the region increased from  $2 \times 10^{-9} \text{ sec}^{-2}$  to  $12 \times 10^{-9} \text{ sec}^{-2}$  (Figs. 14a and 14b), however the maximum values remained with the deepening upper-level trough at 500 mb behind the surface system.

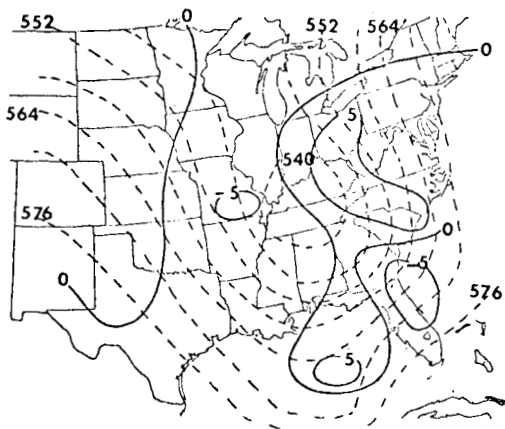
By 0000 GMT on 3 November, the surface cyclone had intensified and had moved from the Gulf of Mexico to Virginia. Positive vorticity advection through the eastern United States increased, with values of  $5 \times 10^{-9} \text{ sec}^{-2}$  observed over the low center through the surface trough (Fig. 14c). In the next 24 hours, the cyclone moved across the eastern Great Lakes region and into Canada, as positive vorticity advection decreased through the northeastern United States. On 3 November, anticyclonic development was observed over southern Texas and the western Gulf of Mexico where the advection of 500-mb vorticity was negative behind the upper-level trough (Fig. 14c). Values of negative advection were small over the developing high-pressure center, however. By 0000 GMT on 4 November, the high-pressure system had moved into the south central United States,



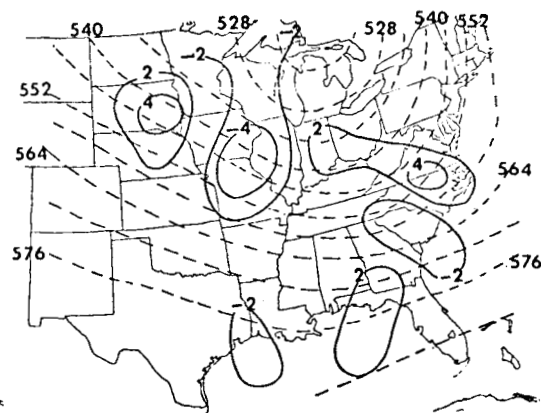
(a) 1 November 1966



(b) 2 November 1966



(c) 3 November 1966



(d) 4 November 1966

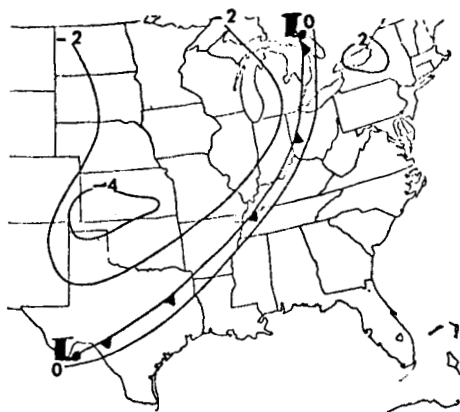
Fig. 14. Charts of 500-mb vorticity advection for 0000 GMT, 1-4 November 1966. (Solid lines indicate 500-mb vorticity advection ( $10^{-9} \text{ sec}^{-2}$ ) and dashed lines represent the 500-mb height contours. Positive values indicate cyclonic advection.)

but development was still relatively weak. The advection of negative vorticity had increased through the region, but magnitudes remained small (Fig. 14d).

## 2) Advection of Thickness (Term III, Eq. (7))

It was demonstrated by the results of the first case (Figs. 6 and 7) that the advection of 1000-500-mb thickness was representative of the advection-of-thickness term, after application of the Laplacian operator and constants. The thickness advection itself is more readily inferred from synoptic charts and presents a smoother pattern, and is shown in Fig. 15 for 0000 GMT, 1-4 November 1966. Again, it is clear that contributions from this term are near zero over the surface cyclone, with positive values ahead and negative values to the rear of the storm.

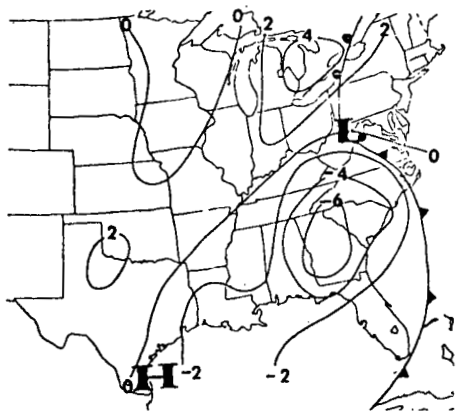
Throughout early stages of cyclone development (Fig. 15a), the gradient of thickness was quite weak and positive and negative values were small. As development increased, magnitudes ahead of and behind the storm increased (Figs. 15b and 15c) and the gradient became larger. On 4 November, as the low center weakened and moved into Canada the gradient of thickness advection around the storm decreased (Fig. 15d). As in the case of cyclone development, the advection of thickness over the developing anticyclone was near zero. Negative values were observed in advance of the system, with positive values behind. As the high-pressure system developed through the south central United States on 3-4 November



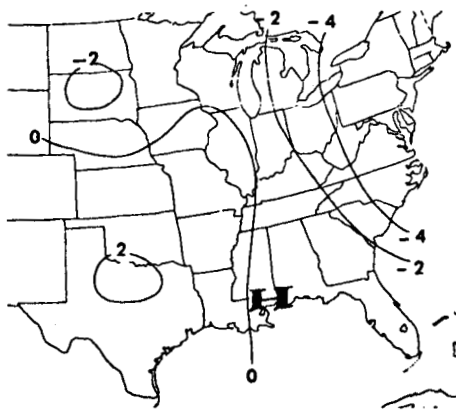
(a) 1 November 1966



(b) 2 November 1966



(c) 3 November 1966



(d) 4 November 1966

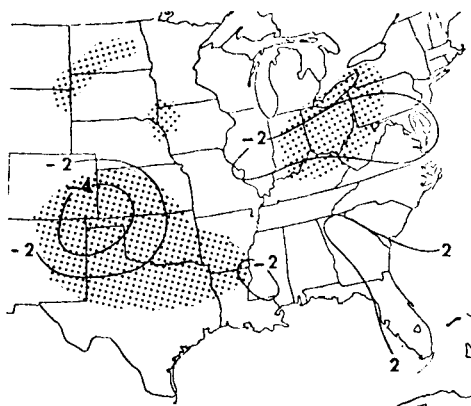
Fig. 15. Charts of 1000-500-mb thickness advection and surface fronts for 0000 GMT, 1-4 November 1966 (units:  $10^{-3}$  m/sec).

(Figs. 15c and 15d), magnitudes of the thickness advection surrounding the anticyclone were small and the gradient was relatively weak.

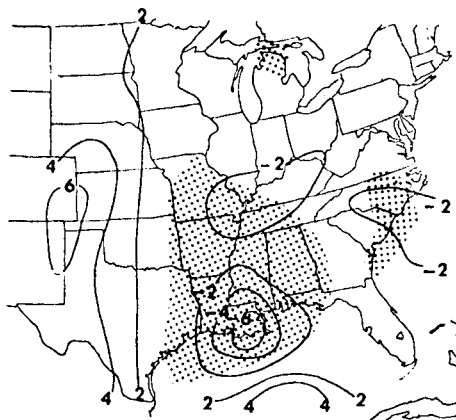
### 3) Stability (Term IV, Eq. (7))

The results of the analysis for the December case demonstrated that patterns of the stability before application of the Laplacian operator and constants were representative of stability patterns after application of the Laplacian operator as shown in Figs. 8 and 9. The stability itself possessed a less cellular configuration and is easier to interpret from customary synoptic analyses. Therefore, stability for 0000 GMT, 1-4 November 1966 is shown in Fig. 16. Throughout initial stages of the cyclone development, instability contributions were small (Fig. 16a). As development intensified and the cyclone center moved from Texas through the Gulf of Mexico to the Virginias (Figs. 16b and 16c), instability reached a maximum. By 4 November, the weakening low system had moved into Canada and stability increased through the Northeastern United States behind the low center (Fig. 16d).

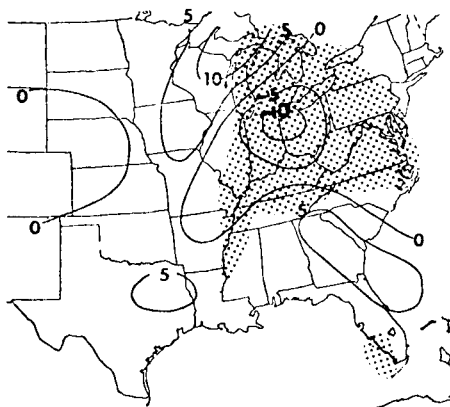
The stability term appears to be critical in the case of anticyclone development. High pressure developed over Texas and the western Gulf of Mexico as stability increased throughout the area (Figs. 16b and 16c). By 0000 GMT on 4 November, stability increased over the surface ridge. Contributions from the advection of 1000-mb vorticity and the vertical transport of vorticity through



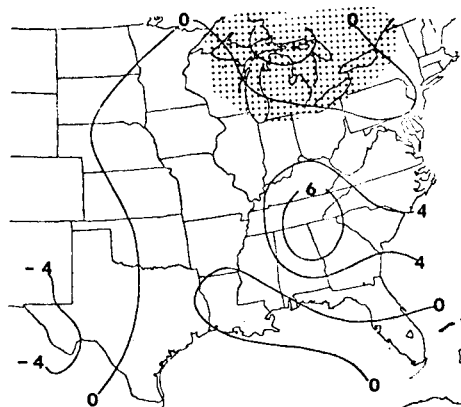
(a) 1 November 1966



(b) 2 November 1966



(c) 3 November 1966



(d) 4 November 1966

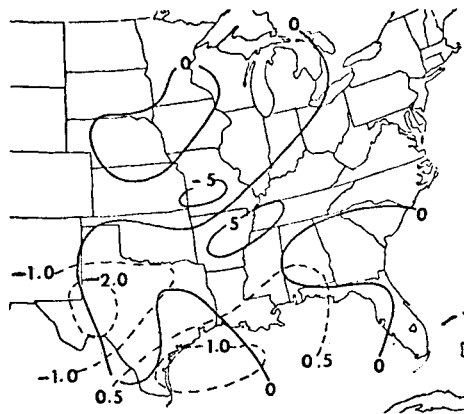
Fig. 16. Comparison of analyses of stability and severe weather activity for 0000 GMT, 1-4 November 1966. (Solid lines indicate stability contours and stippled areas correspond to severe weather echoes reported on NMC radar summaries.)

the LND again were small, with values approximately one order of magnitude less than other contributions.

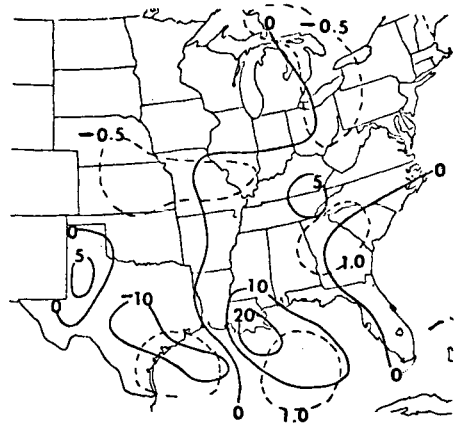
Figure 17 depicts the patterns of the computed and observed tendencies of vorticity at 1000 mb for 0000 GMT. On 1 November, cyclonic tendencies increased through the Gulf of Mexico and the southeastern United States as the low center moved eastward from Texas to the eastern Gulf (Figs. 17a and 17b). By 3 November, cyclonic tendency is seen through the southern Great Lakes and New England corresponding to the movement of the low center to Virginia. To the south of the low, over the southern United States, anticyclonic tendencies confirm the development of high pressure over the western Gulf of Mexico (Figs. 17b and 17c). By 4 November, the cyclonic vorticity tendency had decreased following the movement of the surface low into Canada. Meanwhile, over the southern portion of the country, anticyclonic tendency decreased as development of the high-pressure ridge, centered over Mississippi, was retarded (Fig. 17d).

The patterns of the 1000-mb vorticity tendency, computed by use of terms II, III, and IV in Eq. (7), with the diabatic influence (term V) neglected, indicated general agreement with those observed; however the magnitudes of the computed values again are exaggerated.

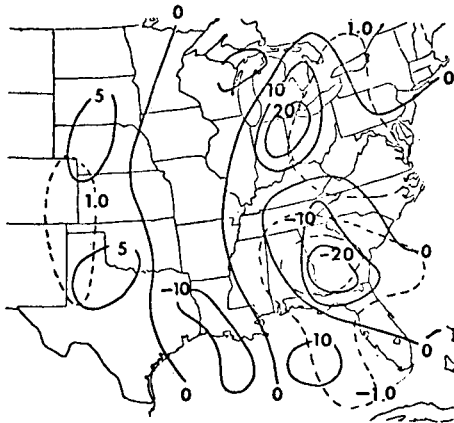
Figure 18 shows the time profiles for the advection of 500-mb vorticity and the stability term over the developing cyclone center



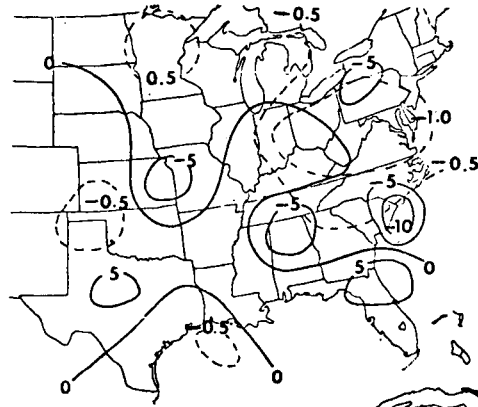
(a) 1 November 1966



(b) 2 November 1966

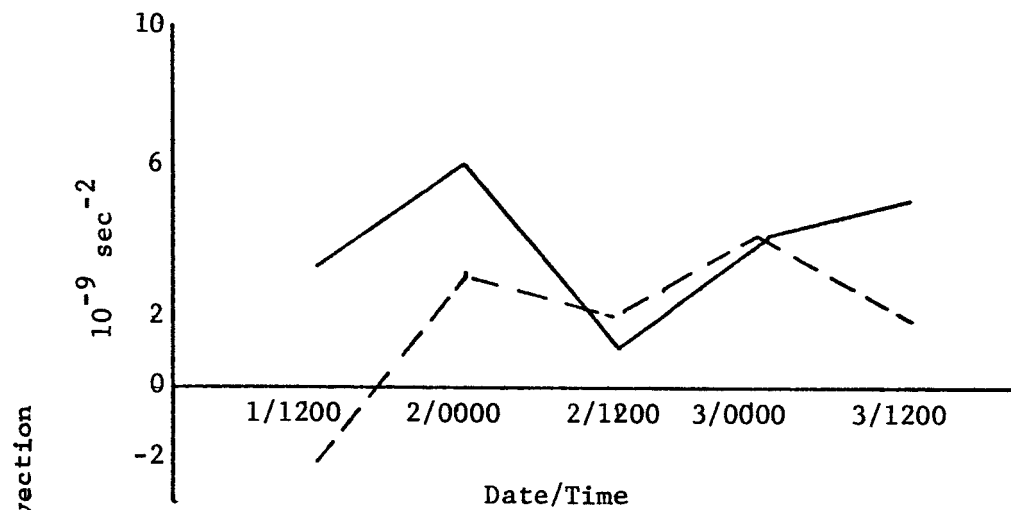


(c) 3 November 1966

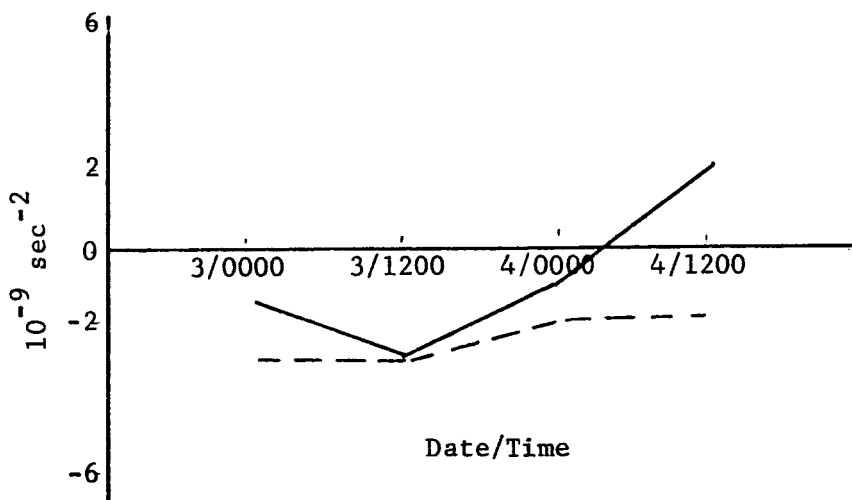


(d) 4 November 1966

Fig. 17. Comparison of the computed vorticity tendency and observed vorticity tendency for 0000 GMT, 1-4 November 1966. (Solid lines indicate contours of the computed tendency ( $10^{-9} \text{ sec}^{-2}$ ) and dashed lines show patterns of the observed tendency ( $10^{-9} \text{ sec}^{-2}$ ). Positive values correspond to cyclonic development and negative values indicate anticyclonic development.)



(a) Cyclonic development, 1-3 November 1966



(b) Anticyclonic development, 3-4 November 1966

Fig. 18. Time profiles of the 500-mb vorticity advection and the stability term over the developing system, for (a) cyclonic development, 1-3 November 1966, and (b) anticyclonic development, 3-4 November 1966. (Solid lines depict the vorticity advection and the dashed lines show the stability term.)

during this synoptic case (Fig. 18a). As indicated, the advection of vorticity at the LND is the dominant factor in early stages of cyclonic development. After development has begun and cloud patterns are formed, the stability term becomes the significant contributor for further development. The time profiles of these terms are shown in Fig. 18b for anticyclone development. The governing influence appears to be the stability term with the advection of negative vorticity acting as an aid. Anticyclonic development is delayed when the latter term becomes more positive, though some development continues.

In summary, the results of these two synoptic cases indicate that the advection of vorticity at 500 mb provides the greatest contribution to cyclonic development during early stages, and that after development has begun, the stability influence becomes significant. Throughout the development process, the advection-of-thickness term remains small over the surface center, with a positive maximum in advance and a negative minimum behind the storm. The diabatic contributions were found to be significant over coastal areas of the Gulf of Mexico and over the Great Lakes.

In both synoptic situations, cyclonic development was most intense when increasing contributions from the advection of vorticity and the stability term coincided above the surface low, and the advection of 1000-500 mb thickness showed a maximum contrast across the center. Development continued to occur until the axis of the

upper trough moved to the east of the surface low center. When this happened, the advection of vorticity decreased over the system and became anticyclonic, thereby opposing the cyclonic contributions of the stability term.

In contrast, anticyclonic development depended primarily on the stability term. The development of high pressure, both positive and negative, proceeded as a result of increasing or decreasing stability, with only small support from the advection of negative vorticity and the thickness advection.

## 5. PRACTICAL UTILIZATION OF RESULTS

### a. Utilization of Facsimile Products

The results of the investigation discussed in previous sections have demonstrated that the Sutcliffe development theory, as modified by Petterssen, provides an understanding of the basic mechanisms involved in cyclonic and anticyclonic development at sea level, over the eastern United States. The problem remains, however, to develop simple forecasting procedures from these results for use by practicing synoptic forecasters. The forecaster must determine areas where positive advection of vorticity at 500 mb and maximum instability coincide with a region of small thickness advection that separates large positive and negative values. The problem is the same for anticyclonic development, except that negative vorticity advection and large stable regions must be located.

The advection of vorticity at 500 mb is obtained readily from vorticity analyses and prognoses that are available to the forecaster twice daily. These facsimile charts, valid at 0000 and 1200 GMT, provide initial contours of the 500-mb vorticity pattern, as well as forecasts for 12, 24, and 36 hours.

The evaluation of thermal quantities also is straightforward. The results of the two test cases indicate that the patterns of the advection of thickness in the layer 1000-500 mb and the pressure-averaged stability are representative of the configurations of these quantities after application of the Laplacian

operator and constants, thereby obviating the necessity of Laplacian determinations.

By use of the NMC 1000-500-mb thickness analyses and forecasts, available at 0000 and 1200 GMT each day, areas of largest positive and negative thickness advection can be located. As an alternate procedure, since the thickness is proportional to the mean virtual temperature of a layer, positive and negative thickness advection are related to warm and cold temperature advection, respectively. These areas also are located easily by use of routine data.

Stability contributions are equally simple to determine. As indicated by Figs. 9 and 16, patterns of reported severe weather on the NMC radar summaries correspond very well with regions of maximum instability. These analyses, provided every 3 hours, may be used to locate maximum stability and instability. The diabatic influence is greatest in association with heat and cold sources, such as the Gulf of Mexico and the Great Lakes. A cyclonic contribution results during the fall and early winter, for example, when the land surrounding the Great Lakes is colder than the water.

b. Forecast Procedures

Based on the two cases considered, the procedures for forecasting the development of cyclones at sea level over the eastern United States may be summarized as follows:

1) Initial development occurs when a region of positive vorticity advection at 500 mb becomes superimposed on an area of large instability, and where a zone of small thickness advection separates large positive and negative areas.

2) Intensification results when the advection of vorticity and thermal quantities increase over the storm.

3) Movement of a developing cyclone proceeds toward the region of maximum positive thickness advection and away from negative thickness advection.

4) A surface cyclone begins to fill when the advection of 500-mb vorticity decreases over the storm and when the temperature contrasts surrounding the storm decrease.

The procedures for forecasting anticyclonic development may be stated as follows:

1) Initial development and growth occurs as a result of the superimposition of small or negative vorticity advection on a region with increasing stability, and where a zone of small thickness advection separates large negative and positive areas.

2) An anticyclone will build when the stability increases and the vorticity advection becomes more negative.

3) The movement of anticyclones is toward the area of greatest stability and also is closely associated to the movement of the upper-level ridge.

4) An anticyclone will cease to develop when the stability begins to decrease within the anticyclone and when the advection of 500-mb vorticity becomes more positive.

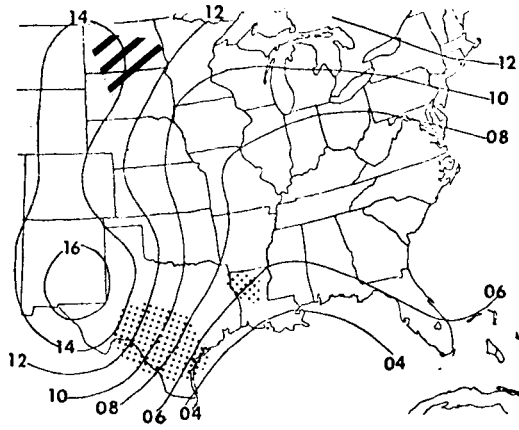
c. Test of the Procedures

As a test of the procedures, the facsimile charts and forecasting rules given above were used to determine the development and movement of a surface cyclone and anticyclone. Figures 19-22 show copies of the NMC analyses for 500-mb vorticity, 1000-500-mb thickness, radar summaries, and surface contours. Stippled areas represent the greatest contributions toward cyclonic development, and hatched areas show the anticyclonic contributions.

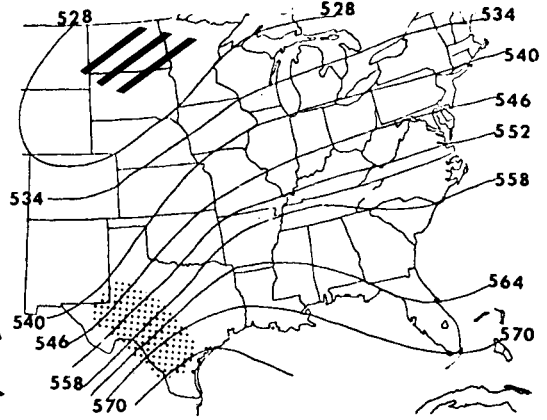
At 1200 GMT on 21 February, positive vorticity is being advected into southern Texas and over Louisiana (Fig. 19a), while the magnitude of the thickness gradient increased over the same region (Fig. 19b). Widely scattered areas of convective activity are indicated by the radar summary at this time (Fig. 19d).

Over North Dakota, the absence of convective activity and the small gradient of the thickness pattern indicates stable conditions, in association with the high-pressure center.

By 0000 GMT on 22 February, advection of positive vorticity is indicated from southern Missouri to Louisiana as positive vorticity spreads eastward into Oklahoma (Fig. 20a). The thickness gradient has increased through the region and convective activity has become more severe (Figs. 20b and 20c); this corresponds to the



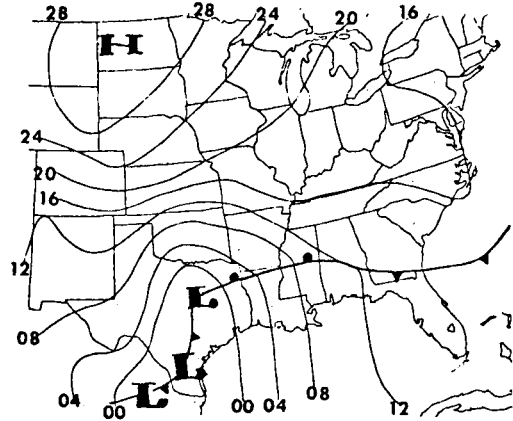
(a) 500-mb vorticity ( $10^{-5} \text{ sec}^{-1}$ )



(b) 1000 - 500-mb thickness analysis

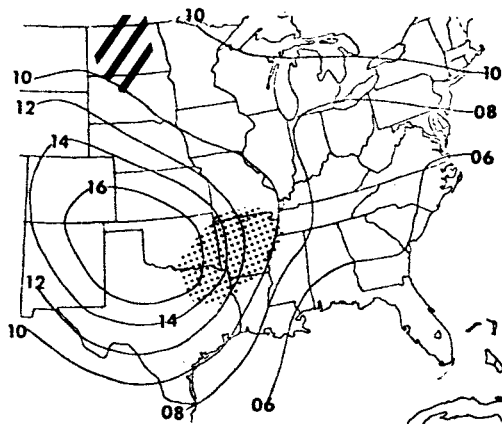


(c) Radar Summary

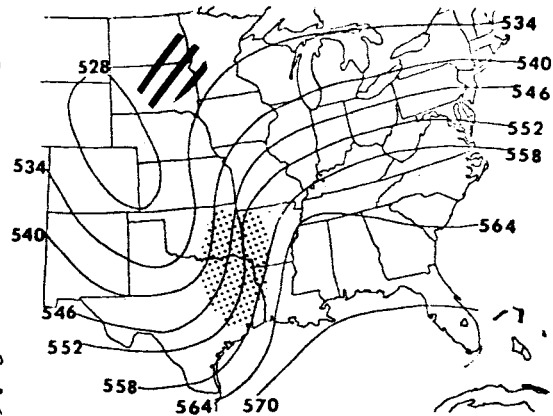


(d) Surface Analysis

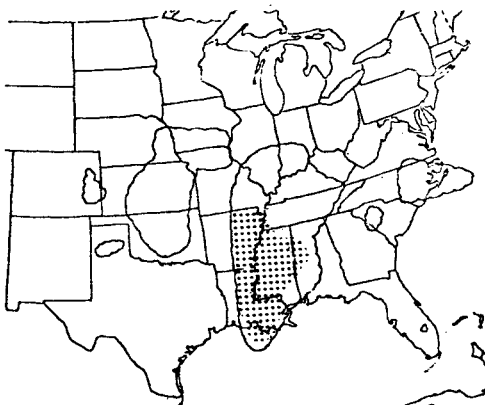
Fig. 19. Copies of the NMC facsimile charts for 1200 GMT, 21 February 1971. (Stippled areas show the cyclonic contributions toward development and hatched areas represent anti-cyclonic contributions.)



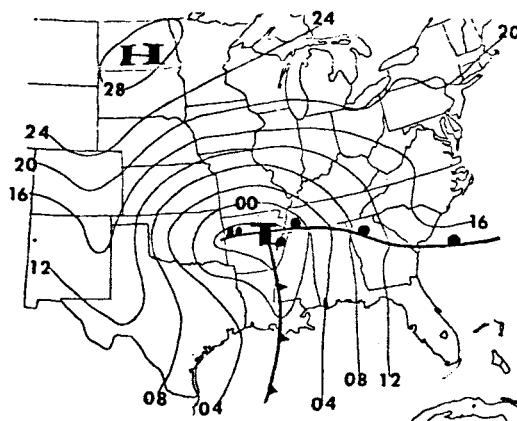
(a) 500-mb vorticity  
( $10^{-5} \text{ sec}^{-1}$ )



(b) 1000-500-mb thickness  
analysis



(c) Radar Summary



(d) Surface Analysis

Fig. 20. Copies of the NMC facsimile charts for 0000 GMT, 22 February 1971. (Stippled areas show the cyclonic contributions toward development and hatched areas represent anticyclonic contributions.)

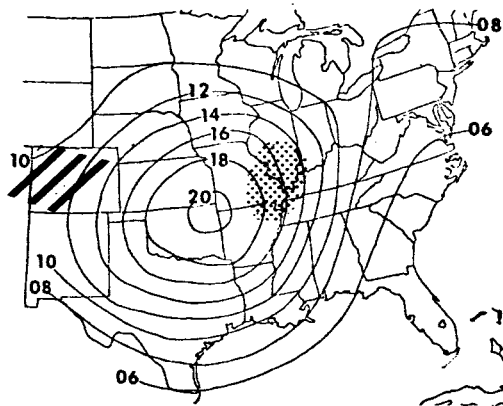
movement of the surface center from Texas to Arkansas (Fig. 20d). Over the north central United States, meanwhile, the high-pressure ridge begins to dissipate as stability and thickness support decrease.

In the next 12 hours, advection of cyclonic vorticity increased rapidly as the low center intensified and moved to Missouri. The 1000-500-mb thickness continued to decrease behind the storm and increase in advance, as convective activity spread through the central United States (Fig. 21).

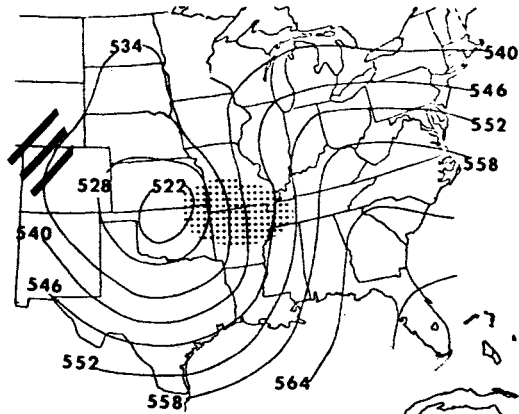
By 0000 GMT on 23 February, the growing center of maximum 500-mb vorticity had moved to Illinois, with the greatest cyclonic advection observed through Kentucky and West Virginia (Fig. 22a), as the surface cyclone became divided into two separate low centers. The 1000-500-mb thickness continued to increase over the northeastern United States and to decrease through the Midwest (Fig. 22b) as stability increased through the central portion of the nation.

The time profile of the 500-mb vorticity over the cyclone center (Fig. 23) corresponds well with the observed life cycle of the low-pressure system which agrees with results determined by the two cases investigated in previous sections (Figs. 11 and 18). Also, the direct dependence of anticyclonic development on stability influences is in concert with results obtained in Section 4.

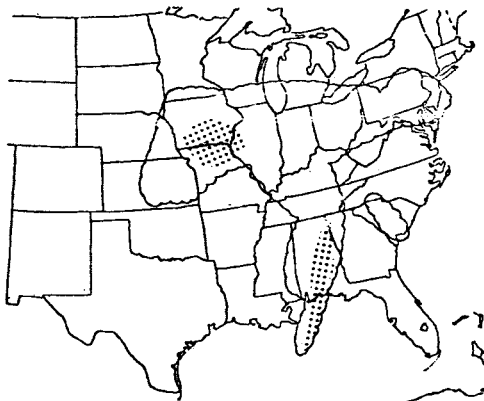
On the basis of this test, it may be concluded that the procedures outlined in this Section provide an acceptable technique



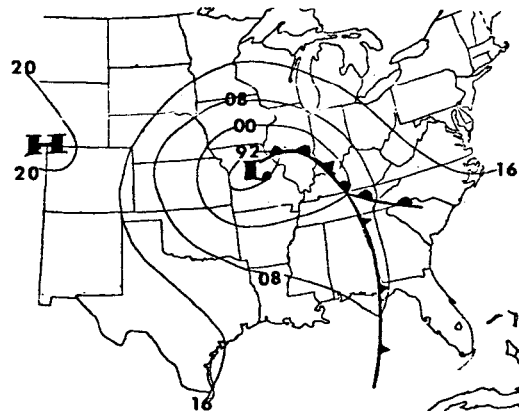
(a) 500-mb vorticity  
( $10^{-5} \text{ sec}^{-1}$ )



(b) 1000-500-mb thickness  
analysis

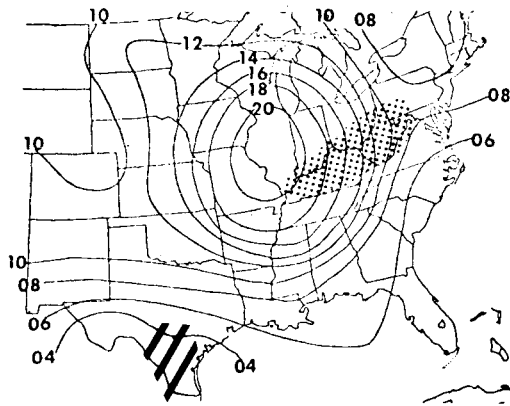


(c) Radar Summary

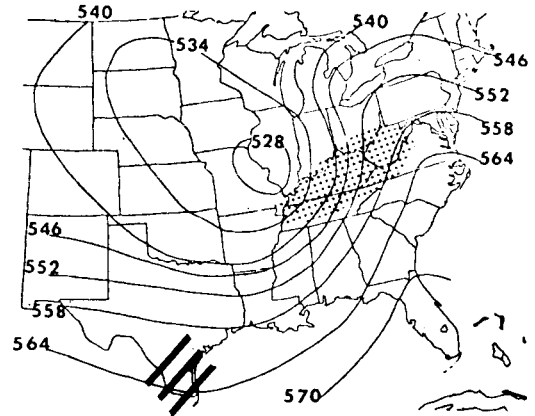


(d) Surface Analysis

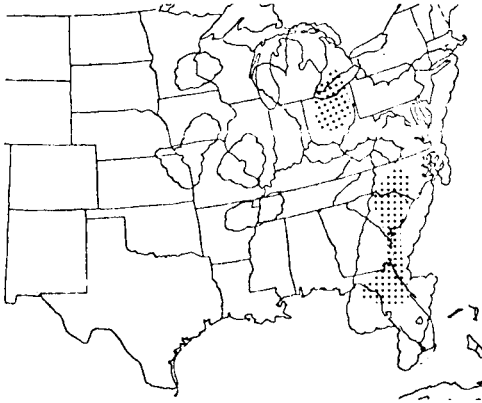
Fig. 21. Copies of the NMC facsimile charts for 1200 GMT 22 February 1971. (Stippled areas show the cyclonic contributions toward development and hatched areas represent anticyclonic contributions.)



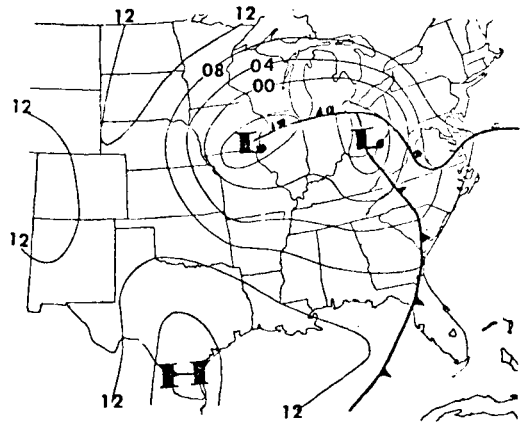
(a) 500-mb vorticity  
( $10^{-5} \text{ sec}^{-1}$ )



(b) 1000-500-thickness  
analysis



(c) Radar Summary



(d) Surface Analysis

Fig. 22. Copies of the NMC facsimile charts for 0000 GMT, 23 February 1971. (Stippled areas show the cyclonic contributions toward development and hatched areas represent anticyclonic contributions.)

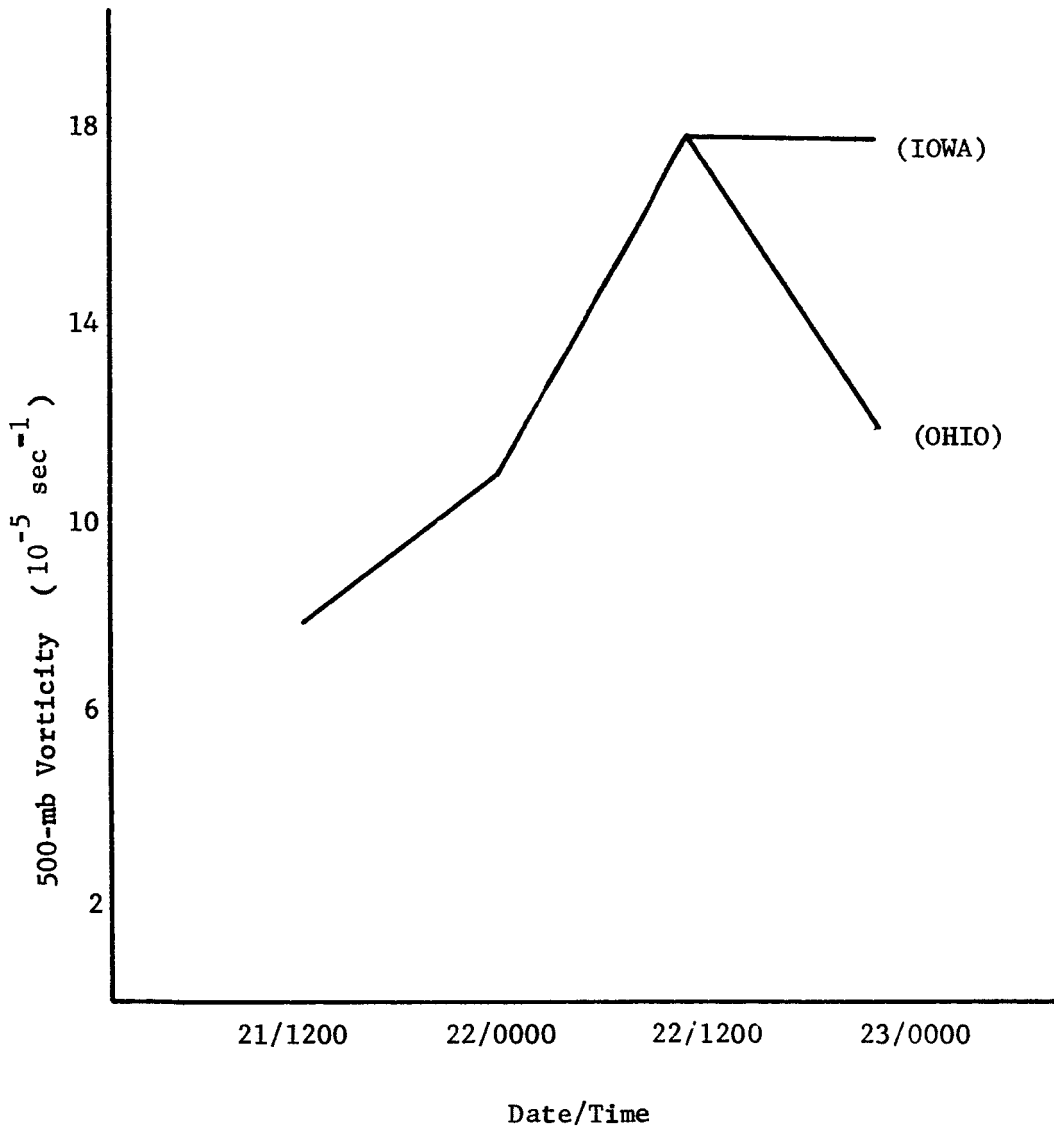


Fig. 23. Time profile of 500-mb vorticity over the cyclone center for 21-23 February 1971.

for forecasting the development and subsequent decay of cyclones and anticyclones over the eastern United States.

## 6. SUMMARY AND CONCLUSIONS

This research is an investigation of the Sutcliffe development theory, as modified by Petterssen. All of the terms, including those assumed to be small and usually neglected by previous investigators, were examined.

A grid system covering the eastern United States was employed and rawinsonde data, checked for hydrostatic consistency, were interpolated to the grid points by successively correcting a first-guess field initialized at zero. Computer programs were written to evaluate the terms in the development equation for two synoptic case studies, providing examples of cyclonic and anticyclonic development, movement, and decay over the eastern United States. Scalar fields of each parameter were analyzed to determine when and where each term made significant contributions to the development process.

Results indicate that the Sutcliffe-Petterssen development theory is a useful tool for the description of cyclonic and anticyclonic development at Earth's surface. It was determined that the dominant influence for the initial development and growth of cyclones is the advection of positive vorticity at the level of non-divergence, and that thermal quantities become predominant after development has begun. Cyclones, it was found, continue to develop until the axis of the upper-level trough moves over the surface

system and the negative advection of vorticity is strong enough to counteract cyclonic contributions from thermal variables.

In contrast, anticyclonic development was primarily influenced by the stability term while the advection of vorticity at the level of non-divergence and other thermal quantities provided only weak assistance.

Contributions from the advection of 1000-mb vorticity and the vertical transport of vorticity through the level of non-divergence were found to be substantially smaller than other contributions and may be neglected. This confirms the conclusions of previous investigators.

Patterns of the tendency of vorticity at 1000 mb, computed by use of Petterssen's development equation, compare well with observed patterns of the tendency of 1000-mb vorticity and with observed development. The magnitudes are considerably exaggerated, however.

Simple procedures for forecasting the development and movement of cyclones and anticyclones were formulated. The rules, based on fundamental techniques, depend on routinely available data, and a test of these procedures showed that they are accurate and easily applied.

## 7. RECOMMENDATIONS FOR FURTHER RESEARCH

Research based on the Sutcliffe development theory should continue. This investigation was confined to the development of cyclones and anticyclones over the eastern United States during winter, and the results are strictly valid only for these conditions. Many more cases should be investigated using examples of both cyclonic and anticyclonic development for other seasons and for different parts of Earth. It is suspected that over the Sea of Japan during winter, for example, the thermal quantities will be more important during initial cyclonic development. As another example, anticyclones moving from the North American continent over the North Atlantic Ocean in winter are observed to undergo increased development thereby indicating the important effect of the diabatic term. This effect should be studied in greater detail.

The forecast procedures outlined in this paper should be systematically and routinely applied in the weather station and forecast center and alternate techniques devised. In addition, practical methods for forecasting upper-level winds, clouds, temperatures, and severe weather activity could be developed by extending the procedures outlined in this investigation.

## REFERENCES

- Barnes, S. L., 1964: A technique for maximizing details in numerical weather map analysis. J. Appl. Meteorol., 3, 396-409.
- Bradbury, D. L., 1957: An experiment in stability and moisture analysis. Final Rept., Air Force Contract AF 19(604)-1293, Art. H, Dept. of Meteorol., University of Chicago, 32pp.
- Breistein, P. M., 1954: Investigation of cyclone development, storm 2. Tech. Rept. 6, Air Force Contract AF 19(604)-390, Dept. of Meteorol., University of Chicago, 19pp.
- Brodrick, H. J. and E. P. McClain, 1969: Synoptic/dynamic diagnosis of a developing cyclone and its satellite-viewed cloud patterns. ESSA Tech. Rept. NESC-49, Washington, D. C., 26pp.
- Byers, H. R., 1959: General Meteorology, New York, McGraw-Hill Book Company, Ch. 17.
- Estoque, M. A., 1956: A prediction model for cyclone development integrated by Fjortoft's method. J. Meteorol., 13, 195-202.
- \_\_\_\_\_, 1957a: Graphical integrations of a two-level model. J. Meteorol., 14, 38-42.
- \_\_\_\_\_, 1957b: The mechanism of vorticity change associated with a selected cyclone. Final Rept., Air Force Contract AF 19(604)-1293, Art. P., Dept. of Meteorol., University of Chicago, 29pp.
- Hess, S. L., 1959: Introduction to Theoretical Meteorology, New York, Holt, Rinehart and Winston, 92-100.
- Means, L. L., 1955: An investigation of cyclone development, storm 13-15 December 1951. Mon. Wea. Rev., 83, 185-198.
- Newton, C. W., 1956: Mechanisms of circulation change during a lee cyclogenesis. J. Meteorol., 13, 528-539.
- Panofsky, H., 1964: Introduction to Dynamic Meteorology, University Park, The Pennsylvania State University Press, 80-92.
- Petterssen, S., 1955: A general survey of factors influencing development at sea level. J. Meteorol., 12, 36-42.

\_\_\_\_\_, 1956: Weather Analysis and Forecasting, Vol. 1, McGraw-Hill Book Company, 428pp.

\_\_\_\_\_, and D. L. Bradbury, 1954: An investigation of cyclone development, storm 1. Tech. Rept. 5, Air Force Contract AF 19(604)-390, Dept. of Meteorol., University of Chicago, 68pp.

\_\_\_\_\_, G. E. Dunn, and L. L. Means, 1955: Report of an experiment in forecasting of cyclone development. J. Meteorol., 12, 58-67.

Sutcliffe, R. C., 1939: Cyclonic and anticyclonic development. Quart. J. Roy. Meteorol. Soc., 65, 518-524.

\_\_\_\_\_, 1947: A contribution to the problem of development. Quart. J. Roy. Meteorol. Soc., 73, 370-383.

\_\_\_\_\_, and A. G. Forsdyke, 1950: The theory and use of upper air thickness patterns in forecasting. Quart. J. Roy. Meteorol. Soc., 76, 189-217.

## THE ISOBARIC VORTICITY EQUATION

The quantity  $Q$  in Eq. (1) on page 2 is the local vertical component of the isobaric vorticity vector of an air particle relative to an inertial frame of reference. The quantity  $Q$  is related to the local vertical component of the relative isobaric vorticity vector through the equation

$$Q = \left( \frac{\partial v}{\partial x} \right)_p - \left( \frac{\partial u}{\partial y} \right)_p + 2\Omega \sin \theta, \quad (\text{A-1})$$

where the first two terms on the right hand side together denote the local vertical component of the relative isobaric vorticity vector, i.e., the isobaric vorticity relative to a frame of reference attached to the surface of the earth. The quantities  $u$  and  $v$  denote the easterly and northerly components of wind and  $\Omega$  and  $\theta$  denote the angular velocity of the earth and latitude of the origin of the relative frame of reference. The subscript  $p$  on the partial derivatives in the above equation means that these derivatives are evaluated in an  $x, y, p, t$  coordinate system, where  $x$  and  $y$  denote east-west and north-south coordinates. The elimination of height  $z$  in favor of  $p$  occurs through the assumption that the atmosphere is hydrostatic, so that

$$\frac{\partial p}{\partial z} = -\rho g, \quad (\text{A-2})$$

where  $\rho$  and  $g$  denote density and gravity. This permits the horizontal equations of motion to be expressed as

$$\left( \frac{\partial u}{\partial t} \right)_p + u \left( \frac{\partial u}{\partial x} \right)_p + v \left( \frac{\partial u}{\partial y} \right)_p + w \frac{\partial u}{\partial p} = -g \left( \frac{\partial z}{\partial x} \right)_p + fv, \quad (\text{A-3})$$

\*Prepared by George H. Fichtl, Aerospace Environment Division, Marshall Space Flight Center, NASA.

$$\left(\frac{\partial v}{\partial t}\right)_p + u\left(\frac{\partial v}{\partial x}\right)_p + v\left(\frac{\partial v}{\partial y}\right)_p + w\frac{\partial v}{\partial p} = -g\left(\frac{\partial z}{\partial y}\right)_p - fu, \quad (\text{A-4})$$

where  $f = 2\Omega \sin \theta$  and

$$w = \frac{dp}{dt}. \quad (\text{A-5})$$

The quantity  $w$  is sometimes called p-velocity and may be approximated by  $-\rho gw$ , where  $w$  is the vertical velocity of the air. It should be noted that  $z$  in equations (A-3) and (A-4) is the height of a pressure surface and is now a dependent variable, while  $p$  is now an independent variable.

If we operate on (A-4) with  $\left(\frac{\partial}{\partial x}\right)_p$  and (A-3) with  $\left(\frac{\partial}{\partial y}\right)_p$  and subtract the resulting relationships, we obtain the isobaric vorticity equation for  $Q$ :

$$\frac{dQ}{dt} = -QD + \left(\frac{\partial w}{\partial y}\right)_p \frac{\partial u}{\partial p} - \left(\frac{\partial w}{\partial x}\right)_p \frac{\partial v}{\partial p}, \quad (\text{A-6})$$

where  $D$  is the isobaric horizontal divergence

$$D = \left(\frac{\partial u}{\partial x}\right)_p + \left(\frac{\partial v}{\partial y}\right)_p \quad (\text{A-7})$$

$$\text{and } \frac{d}{dt} = \left(\frac{\partial}{\partial t}\right)_p + u\left(\frac{\partial}{\partial x}\right)_p + v\left(\frac{\partial}{\partial y}\right)_p + w\frac{\partial}{\partial p}. \quad (\text{A-8})$$

It should be noted that (A-6) is identical in form to the equation for the vertical component of vorticity in an  $x, y, z, t$  coordinate system for a barotropic atmosphere; however (A-6) is valid for both barotropic and baroclinic atmospheres. The last two terms on the right-side of (A-6) are analogous to the vortex-tube terms in the vorticity equation in an  $x, y, z, t$  system and can be neglected through scale analysis considerations.

Now the equation of mass continuity in an  $x, y, z, t$  system is given by

$$\frac{\partial u}{\partial x} + \frac{\partial v}{\partial y} + \frac{\partial w}{\partial z} = - \left[ \frac{\partial \rho}{\partial t} + u \frac{\partial \rho}{\partial x} + v \frac{\partial \rho}{\partial y} + w \frac{\partial \rho}{\partial z} \right]. \quad (\text{A-9})$$

Transformation of this equation to the  $x, y, p, t$  coordinate system yields

$$\left( \frac{\partial u}{\partial x} \right)_p + \left( \frac{\partial v}{\partial y} \right)_p + \frac{\partial w}{\partial p} = 0. \quad (\text{A-10})$$

This equation is identical in form to the equation of mass continuity in an  $x, y, z, t$  system for an incompressible fluid, i.e.

$$\frac{\partial u}{\partial x} + \frac{\partial v}{\partial y} + \frac{\partial w}{\partial z} = 0, \quad (\text{A-11})$$

so that transformation to  $x, y, p, t$  coordinates produces mathematical simplification. The elimination of  $D$  from (A-6) with (A-10) and neglect of the vortex-tube terms permits the isobaric vorticity equation to be expressed in the form

$$\frac{dQ}{dt} = Q \frac{\partial \omega}{\partial p}. \quad (\text{A-12})$$

Further simplification can be obtained by neglecting the vertical advection term  $w \partial Q / \partial p$  against the horizontal advection terms  $u (\partial Q / \partial x)_p$  and  $v (\partial Q / \partial y)_p$ , a reasonable assumption for synoptic scale flows.

How is vertical components of isobaric vorticity and vorticity in  $x, y, z, t$  system related? It can be shown that subject to the differential transformation (A-2)

$$\left( \frac{\partial}{\partial x} \right)_p = \left( \frac{\partial}{\partial x} \right)_z + \left( \frac{\partial z}{\partial x} \right)_p \left( \frac{\partial}{\partial z} \right), \quad (\text{A-13})$$

$$\left(\frac{\partial}{\partial y}\right)_p = \left(\frac{\partial}{\partial y}\right)_z + \left(\frac{\partial z}{\partial y}\right)_p \frac{\partial}{\partial z}, \quad (\text{A-14})$$

where  $(\partial \xi / \partial x)_p$  and  $(\partial \xi / \partial y)_p$  denote horizontal space changes of a variable  $\xi$  in a pressure surface. The quantities  $(\partial z / \partial x)$  and  $(\partial z / \partial y)_p$  denotes the east-west, and north-south slopes of the pressure surfaces.

Substitution of (A-13) and (A-14) into (A-1) yields

$$Q = \left(\frac{\partial v}{\partial x}\right)_z - \left(\frac{\partial u}{\partial y}\right)_p + 2\Omega \sin \theta + \left(\frac{\partial z}{\partial x}\right)_p \frac{\partial v}{\partial z} - \left(\frac{\partial z}{\partial y}\right)_p \frac{\partial u}{\partial z}. \quad (\text{A-15})$$

The first three terms on the right-hand side of (A-15) together constitute the vertical component of the vorticity vector relative to an inertial frame, so that the difference between the isobaric vertical vorticity and vertical vorticity in an  $x, y, z, t$  system is given the last two terms on the right-hand side of (A-15).